Review Article

Yishan Li[#], Lijie Huang*[#], Xiyue Wang, Yanan Wang, Xuyang Lu, Zhehao Wei, Qi Mo, Yao Sheng, Shuya Zhang, Chongxing Huang, and Qingshan Duan

Blending and functionalisation modification of 3D printed polylactic acid for fused deposition modeling

https://doi.org/10.1515/rams-2023-0140 received July 20, 2023; accepted October 16, 2023

Abstract: Polylactic acid (PLA) is extensively used as a raw material in fused deposition modeling (FDM)-based threedimensional printing (3DP), owing to its abundant resources, simple production processes, decent biodegradability, and adequate mechanical strength. However, it has disadvantages such as poor toughness and straightforward bending deformation. Given the considerable application potential of PLA materials in FDM-based 3DP technology, herein, studies conducted over the last 5 years toward the enhancement of the characteristics of PLA for FDM are summarized. In particular, modification approaches (chemical or physical methods) that have been employed to improve the mechanical and processing attributes of PLA are discussed, along with the development of PLA composites with unique functionalities. The insights provided herein can help expand the scope of application of PLA composites in FDM-based 3DP for utilization in fields such as transportation, aerospace engineering, industrial equipment fabrication, consumer/electronic product manufacturing, and biomedicine/medicine.

Keywords: polylactic acid, fused deposition molding, 3D printing, mechanical properties

Yishan Li, Xiyue Wang, Yanan Wang, Xuyang Lu, Qi Mo, Yao Sheng, Shuya Zhang, Chongxing Huang, Qingshan Duan: College of Light Industry and Food Engineering, Guangxi University, Nanning 530004, China

Zhehao Wei: Guangxi Key Laboratory of Clean Pulp and Papermaking and Pollution Control, College of Light Industry and Food Engineering, Guangxi University, Nanning 530004, China

1 Introduction

Additive manufacturing is an advanced manufacturing solution that mainly includes extrusion-based three-dimensional printing (3DP) techniques, powder-based laser sintering, and stereolithography (SLA) [1]. 3DP is an additive manufacturing-based rapid prototyping technology that has been widely used in multidisciplinary fields including biomedicine, aerospace engineering, mechanical design, and industrial manufacturing. Fused deposition modeling (FDM) is one of the extensively used techniques in 3DP, different from other 3DP techniques such as selective laser sintering, SLA, 3DP, and laminated object manufacturing [2], extensively employed as a highly flexible, cost-effective 3DP technology that allows for flexible control of printing parameters such as temperature, layer height, and fill density [3]. FDM is used to create precisely printed molten filaments and to enable layer-by-layer stacking through modeling. In recent years, there has been a gradual increase in research on the use of polylactic acid (PLA) for FDM (Figure 1). Compared to similar products manufactured using conventional techniques such as injection molding or hot pressing, the developed PLA-based composites can be used for the production of end-products manufactured using FDM technology, despite the reduction in mechanical properties [4].

PLA is a degradable plastic that has been comprehensively researched and applied in numerous fields. Its raw materials include renewable plant fibers, corn, sugar cane, and agricultural byproducts. PLA is also nontoxic and environmentally friendly owing to its high biodegradability and tendency to decompose naturally in approximately 3–6 months. Additionally, PLA can replace polypropylene (PP) and polyethylene terephthalate in certain fields owing to its excellent thermomechanical properties (tensile strength: \sim 50 MPa; melting point ($T_{\rm m}$): 180°C; glass transition temperature ($T_{\rm g}$): 60°C). It also has decent gloss, transparency, hand feel, and moderate antibacterial properties. However, it has disadvantages such as poor impact performance, low

[#] These authors contributed equally to this work and should be considered first co-authors.

^{*} Corresponding author: Lijie Huang, College of Light Industry and Food Engineering, Guangxi University, Nanning 530004, China, e-mail: jiely165@qxu.edu.cn

2 — Yishan Li et al. DE GRUYTER

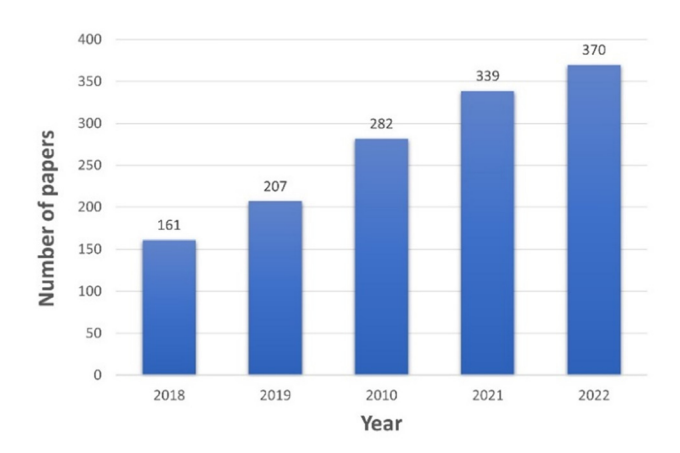


Figure 1: Number of published papers on the use of PLA in FDM over the last 5 years.

toughness, hard and brittle texture, and low heat resistance owing to the rigidity of its molecular chains and crystallization-related difficulties. Regarding its chemical structure, PLA lacks reactive functional groups and is not hydrophilic; therefore, it must be modified to improve its mechanical properties and processing performance.

This article reviews the literature on FDM of PLA materials over the last 5 years. Existing PLA modification processes typically involve the selection of a suitable modifier for reacting with PLA and a method that facilitates this reaction to produce a composite with enhanced mechanical properties and heat resistance. Commonly used modifiers include polycaprolactone (PCL), polyethylene glycol (PEG), natural rubber (NR), and certain aliphatic polymers. Additionally, materials with the shape-memory functionality such as polyurethane (PU), polyvinyl acetate, and multiwalled carbon nanotubes (MWCNTs) can be compounded with PLA to develop products with shape memory for 3DP. Furthermore, nanoparticles can also be used to modify PLA owing to their small size, high specific surface area, and strong interfacial bonding, to generate PLA composites with excellent properties. Using suitable modification methods, FDMbased 3DP PLA materials can be prepared at low costs and their overall performance can be improved, allowing their application in the packaging industry as well as the transportation, biomedical, electronic, and electrical fields.

2 PLA modification methods for 3DP

Chemical modification and physical blending are the main PLA modification methods that produce different PLA composites for 3DP. Despite advances in modified PLA materials with improved mechanical properties and functionalities, FDM-based 3DP continues to have disadvantages such as the high surface roughness induced by the layer-by-layer deposition of molten materials. In terms of practical applications, a poor surface finish can lead to large tolerances and limit the functionality of the FDM-derived parts. Consequently, different postprocessing methods such as laser polishing, microwave heating, mechanical polishing, chemical polishing, and pearlescent treatment have been developed to improve the surface finish of FDM-derived parts. Figure 2 shows the modification and post-processing methods used for 3DP PLA.

Physical blending methods can accommodate numerous raw materials and are simple to operate. Chemical modification processes can be designed and implemented effectively as required; however, they are comparatively tedious and more expensive than physical blending methods. Therefore, the discovery of low-price, abundantly available filler materials and the establishment of novel synthesis routes have drawn considerable industrial attention for the development of new pathways to obtain PLA composites with superior overall performance.

2.1 Chemical modification

Chemical modification methods such as copolymerization, chain expansion, and crosslinking involve combining reactive groups/monomers and PLA through the formation of covalent bonds with a relatively strong binding force. Diverse functionalized side groups (such as carboxyl, amino, and hydroxyl) can be introduced into the chains of PLA to

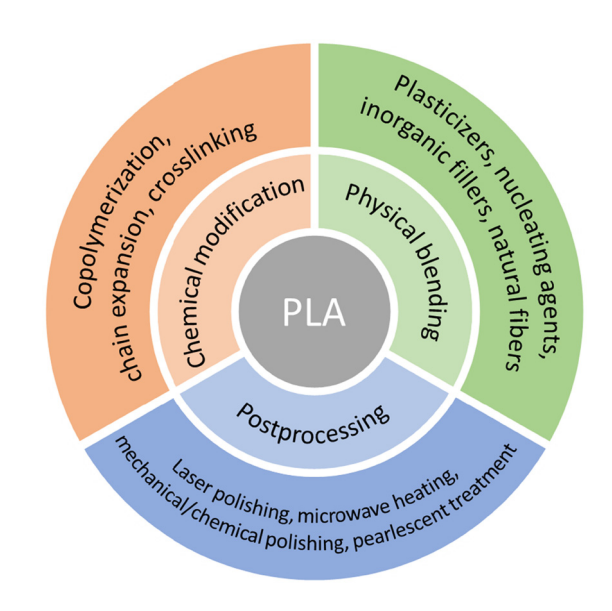


Figure 2: Modification and posttreatment methods for 3DP PLA.

alter its chemical or surface structures and to permanently modify the surface of PLA, so as to achieve the effect of improving the mechanical properties, hydrophobicity, brittleness, and degradation rate [5].

2.1.1 Copolymerization

Because PLA is hydrophobic and its degradation cycle is intractable, it is often copolymerized with other monomers to modify its hydrophobicity and crystallinity and to control its degradation rate. The modification is based on the molecular weight of the copolymer and the type and content ratio of the copolymerized monomers.

The synthesis of PLA copolymers with different compositions and specific structures has received increasing attention, because desired functional groups or related polymer segments have bestowed PLA with special properties by combining the advantages of various groups. These segments have been introduced into the PLA macromolecular chains through free-radical, ionic addition, ring-opening polymerization, or copolymerization. Copolymerization is an effective approach for obtaining polymeric materials with unique properties. By adjusting the molecular structure and order of the combination of the copolymer monomers, the lactic acid/other-monomer ratio can be modified, thus improving the mechanical properties, crystallization attributes, and hydrophobicity of the materials. Copolymerization-based PLA modification is typically achieved by forming linear copolymers using reasonably hydrophilic PEG, polyglycolic acid, PCL, and other chain segments or by preparing graft copolymers using polysaccharide compounds and polymethacrylic acid.

2.1.2 Chain expansion

In this modification method, other molecular chains or active functional groups are introduced into the PLA molecular chains to increase their end length and alter their microstructure, which can effectively resolve the performance issues of PLA materials. Moreover, viscosity increases with increasing molecular weight of the complex formed via chain expansion. For example, the use of styrene and acrylic acid epoxy copolymer [6] as chain extenders can improve the crystallinity and chain segment irregularity of PLA.

2.1.3 Crosslinking

In this process, the properties of PLA are improved by crosslinking it with other monomers under the action of crosslinking agents or radiation to create a polymer network. For instance, 2,2,6,6-tetramethyl-1-piperidinyloxy (TEMPO)-oxidized bacterial cellulose (TOBC) has been used to reinforce PLA. Homogeneously dispersing TOBC in the PLA matrix helps form a three-dimensional (3D) network and crosslinked structure [7] with a higher tensile strength than that of pristine PLA.

2.2 Physical blending

This PLA modification approach mainly involves blending materials primarily by melt extrusion or solution coating to prepare PLA composites. In contrast to copolymerizationbased modification, blending is a more targeted approach to improving some of the physical and mechanical properties of a defective polymer, while maintaining its original excellent properties. Moreover, blending is simpler and more economical than chemical modification methods; thus, it is employed extensively for PLA modification. For example, the hydrophilicity of PLA can be improved by blending it with materials including acrylic acid, starch, and PCL. The most commonly used blending method is melt blending. PLA composites can be prepared according to the types of the blend components such as plasticizers, nucleating agents, inorganic fillers, natural fibers, or other degradable materials.

2.2.1 Plasticizer blending

PLA is a hard, brittle material with a high elastic modulus. Plasticizer-based modification involves using certain nonvolatile, high-boiling-point chemicals that can enhance the mechanical properties and processing performance of PLA. Common plasticizers include citrates, glucose ethers, propanetriol, and PEG. Tributyl citrate (TBC) [8] is a highly safe, nontoxic plasticizer with decent resistance to light, heat, bacteria, and weather, resulting in its use in food packaging. The addition of plasticizers reduces the $T_{\rm g}$ of PLA composites as well as improves their flexibility, impact resistance, and elongation properties. Appropriate plasticizers should be selected to yield the desired composites, as each plasticizer exhibits different effects.

2.2.2 Blending with nucleating agents

Nucleating agents can affect the crystallization behavior of polymer resins by influencing the nucleation point at

which crystallization is initiated, thereby enabling control over certain physical and mechanical properties. Although PLA can crystallize, it has a relatively inferior degree of crystallinity and an extremely wide molecular weight distribution. The use of nucleating agents in conjunction with annealing processes to enhance crystallinity can improve the heat resistance and mechanical properties of PLA [7,9].

2.2.3 Blending with inorganic fillers

Kaolin and montmorillonite are layered silicates that can be compounded with PLA to form PLA/layered silicate nanocomposites [10,11]. Calcium carbonate [12,13] and hydroxyapatite (HAp) can be used as PLA fillers to improve the elongation at break, impact strength, and thermal decomposition temperature of PLA in a cost-effective manner.

2.2.4 Blending with natural fibers

Blending PLA with natural polymers such as cellulose, wood flour (WF), and coconut shells improves its degradability as well as its mechanical properties and thermal stability. Lee $et\ al.$ [14] used natural and kenaf fibers to reinforce PLA and prepare composite filaments for FDM-based 3DP. The fibers used enhanced the strength of the PLA composites, acted as a nucleating agent, and lowered the T_g , resulting in higher flexibility. However, natural fibers also have a negative impact on the mechanical properties: strength always decreases with increasing filler content, while stiffness is essentially the same as the unfilled material at lower filler content but decreases at higher filler content. The elongation at break also decreases, so the proportion of co-mingled has is also critical [15].

2.3 Post-processing

In this step, the FDM-derived products are subjected to heat/laser treatment to improve their smoothness and surface quality.

2.3.1 Laser polishing

This is a new technology that modifies metal and nonmetal surfaces by leveraging the properties of the laser beam interacting with the material. This method has several advantages over traditional polishing techniques. To date, laser polishing – which is a noncontact process – has been employed to modify the surface of parts fabricated using various materials such as glass, diamond, and several metals, which are widely used in important fields such as the automotive, electronics, aviation, and metallurgical industries. Recent advances in additive manufacturing technology have enabled investigation on using laser polishing as a posttreatment technique to improve the surface quality and roughness of additively manufactured parts [16-20]. For instance, re-melting through laser polishing (Figure 3) can be achieved by irradiating a laser beam with a specific energy density and wavelength onto the material, thereby melting/evaporating the surface of the material, which increases its smoothness. This method does not require additional tools and can polish highly complex surfaces that are difficult to accomplish using traditional polishing methods.

2.3.2 Microwave heating

In this method, specimens are heated in a microwave oven. The material at the melt interface is heated by absorbing microwaves. PLA undergoes re-melting at the fusion interface to promote local PLA molecular chain migration and cross-interface entanglement. This weakens the influence of the interface on the specimens, effectively improving their mechanical properties. Wang et al. [21] prepared SiC/PLA composites for FDM-based 3DP and then heated them in a microwave oven, resulting in the absorption of microwaves by SiC at the fusion interface of the specimens. Meanwhile, PLA re-melted at the fusion interface, promoting local PLA chain migration and cross-interface entanglement and thereby weakening the influence of the interface. The results showed that the mechanical properties of the SiC/PLA composites were precisely and effectively improved (Figure 4).

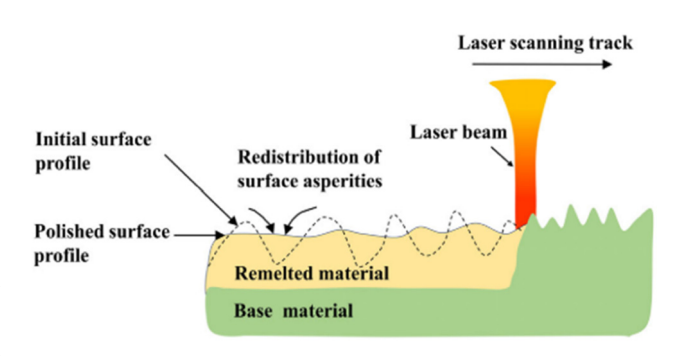


Figure 3: Schematic of the mechanism underlying laser polishing [18].

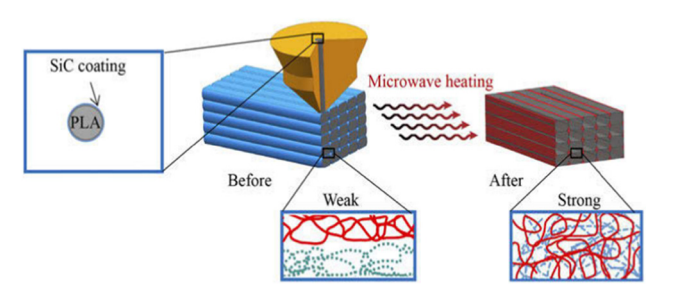


Figure 4: Internal fusion and interfacial distribution in PLA parts obtained through FDM-based 3DP with SiC-coated PLA filaments and microwave heating [21].

2.3.3 Mechanical and chemical polishing

Polishing primarily refers to grinding – that is, eliminating the staircase effect of the molded parts - for satisfying the surface finish and assembly tolerance requirements. In addition to water-wetted sandpaper for direct manual grinding, brushes soaked with 3D model polishing fluid can be used to dissolve and smoothen the surface of molded parts; however, the soaking time and amount being brushed on should be controlled (soaking for 2-5 s at a time or by dipping the brush in 3D model polishing fluid several times).

2.3.4 Pearlescent treatment

In this technique, polishing is achieved by spraying media beads onto the specimen at high-speed using a handheld nozzle. This bead treatment is generally faster than conventional polishing (~5–10 min) and provides products with smoother surfaces, with different generated effects depending on the material.

3 Enhanced modification of PLA for 3DP

3.1 Mechanical property enhancement

Pure PLA-based 3D-printed products are hard, brittle, fragile, and highly susceptible to bending and deformation, limiting their use in the production of structural engineering parts for aerospace or automotive products. Modification of the FDM process [22] and modification of the PLA material are required. The mechanical, frictional, porosity, and thermal properties of pure PLA are usually improved by blending

with other polymers or by adding inorganic fillers; additionally, the compatibility of PLA composites is improved by adding bulking or coupling agents.

3.1.1 Compound modification to improve mechanical properties of PLA

Pure PLA products are typically modified using reinforcements such as carbon fiber (CF), cellulose, and glass fiber to withstand the load-increasing forces during tension and bending, thus improving the strength of the printed products [23-25]. Owing to its attractive characteristics such as lightweight, corrosion resistance, and insulation, PLA is extensively used in industries such as mechanical, chemical, and transportation [26]. Natural polymers such as chitosan (CS) [27] are reasonably compatible with PLA, which inherently exhibits unique physicochemical properties and physiological functions that lead to its noteworthy biocompatibility and functionality. To synthesize biodegradable materials, PLA has also been blended with biodegradable resins to improve its toughness, while retaining its environmental friendliness. Inorganic materials such as silica have also been used as fillers to yield composites with stable functionalities. Furthermore, metals such as copper [28,29] and aluminum [30] have been used to bolster PLA filaments. Adding different fillers to the PLA polymer matrix results in more isotropic FDM parts [31].

Li et al. and Cao et al. [24,32] prepared CF/PLA composites with high mechanical strength using WF. Heidari-Rarani et al. [33] prepared continuous-CF-reinforced PLA composites, which exhibited 36.8 and 109% higher tensile and flexural strengths, respectively, than those of pure PLA. Coppola et al. [34] compounded hemp powder into a biopolymer with PLA and produced composite filaments using a single-screw extruder. The 3D-printed samples exhibited higher elastic modulus and tensile strength than the pure PLA product. Yu et al. [35] modified PLA using coffee grounds to prepare composites whose thermal and mechanical properties were similar and superior, respectively, to those of PLA, thereby reducing the FDM filament fabrication cost and environmental pollution. Li et al. [36] prepared cellulose and glass fibers by TEMPO oxidation and blended them with PLA, yielding hybrid filaments with enhanced impact and tensile strengths.

To preserve its biodegradability in its composites, PLA is typically subjected to melt-blending-based toughening with biodegradable resins. Substances such as polybutylene adipate terephthalate (PBAT), polybutylene succinate (PBS), PCL, and NR can improve the toughness of PLA. Fekete et al. [37] used NR to toughen PLA; it also

significantly improved the ductility of the PLA filaments. Yang et al. [38] prepared a PLA/poly(3-hydroxybutyric acidco-3-hydroxyvalerate) (PHBV) blend, which improved the flowability and toughness of PLA. Wei et al. [39] blended PLA with PCL, and then 3D-printed products with 189% elongation and improved toughness. Enrique Solorio-Rodríguez and Vega-Rios [40] prepared blends of PLA and poly (styrene-co-methyl methacrylate [MMA]), which exhibited a higher Young's modulus, tensile strength, elongation at break, and complex viscosity than those of pure PLA; additionally, the 3D-printed parts did not display vellowing behavior. Kaygusuz and Ozerinc [41] added a polyhydroxyalkanoate (PHA) to PLA to prepare FDM-produced parts with excellent ductility (>160% at 200-240°C); moreover, the elongation at break of the blends was ~40 times higher than that of pure PLA. Han et al. [42] grafted glycidyl methacrylate (GMA) onto PLA chains and exploited the bifunctional properties of GMA to toughen and enhance PLA. At a grafting degree of 10.33%, the mechanical properties and thermal stability of a 25% PLA-GMA/PLA/40% BCB (BCB is defined in this literature as bagasse cellulose passing through a 120 mesh sieve) composite were improved, with the maximum decomposition rate achieved at 355.44°C (Figure 5).

Thermoplastic PU (TPU) materials have decent stability, self-healing, resilience, and mechanical properties [43,44]. Jayswal and Adanur [45] improved the toughness of PLA by adding TPU and found that the elongation at break of the composites increased with increasing TPU

content and that the composites exhibited decent flexibility and strength; this strategy could be applied to 3D-printed flexible-structured plain fabrics. Li *et al.* [46] employed TPU as a modifier to increase the impact toughness of PLA by 631.0%. Dang *et al.* [47] used PP glycerol as the core to synthesize processable star-shaped polyurethane (SPUR) by native prepolymerization and then blended SPUR with PLA to improve the elongation at break, impact strength, and crystallinity of the filament.

Inorganic fillers improve the mechanical properties of PLA while also imparting special properties. Ahmed *et al.* [48] used a silica additive to enhance thermostability and to maximize the quality of PLA/silica in terms of tensile strength (121.03 MPa at 10 wt% silica), toughness (5.6 MPa), ductility (15.3%), and yield stress (63.6 MPa).

The percentage improvements in the mechanical properties of the aforementioned PLA composites with different materials are listed in Table 1.

3.1.2 Additive-based improvements in mechanical properties

When certain materials are directly blended with PLA, composites with inferior mechanical properties are produced owing to issues such as poor interfacial compatibility. Therefore, additives such as coupling agents and compatibilizers are employed to improve the performance of PLA composites.

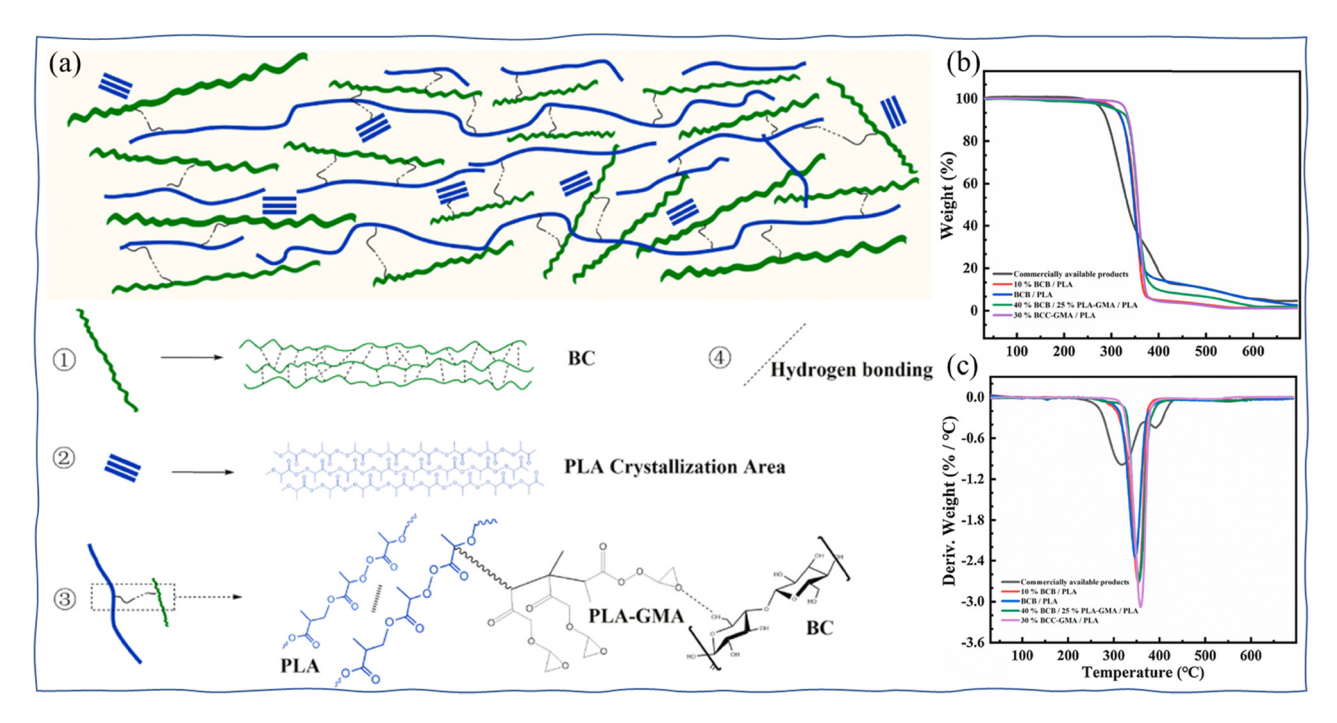


Figure 5: (a) Mechanism of PLA/GMA compatibilization. (b) Thermogravimetry and (c) differential thermogravimetry curves of composites [42].

Table 1: Improvements in the mechanical properties of toughened composites

Composite	Enhancer content	Tensile strength	Elastic modulus	Elongation at break	Flexural strength	Impact strength	Ref.
PLA/CF	/	27%	/	-15.98%	33.33%	15.84%	[24]
PLA/CF	30%	-9.19%	21.15%	24.76%	/	/	[32]
PLA/CCF	/	36.8%	207.8%	/	109%	/	[33]
PLA/hemp	5%	/	64.68%	/	/	/	[34]
PLA/coffee	3%	2.58%	33.24%	/	/	/	[35]
grounds							
PLA/CNF	4-8%	43-52%	/	/	/	34-60%	[36]
PLA/glass fiber	4-8%	54-61%	/	/	/	13-35%	
PLA/NR	20%	-39.28%	29.41%	8361.54%	/	256.77%	[37]
PLA/PHBV	20%	-16.68%	/	33.33%	/	25%	[38]
PLA/PCL	20%	/	/	960%	/	/	[39]
PLA/poly(S-	10%	7.69%	37.93%	-36%	/	/	[40]
co-MMA)							
PLA/PHA	12%	-25%	/	4,000%	/	/	[41]
PLA/GMA	10.33%	-64.92%	-57.19%	4,350.72%	/	/	[42]
PLA/PLA-GMA	25%	95.97%	40.48%	114.01%	/	/	
PLA/PLA-GMA/BCB	40%	121.50%	73.25%	42.25%	/	/	
PLA/TPU	40%	-62.15%	-45.46%	3,192.31%	/	/	[45]
PLA/TPU	40%	/	/	/	/	631.0%	[46]
PLA/SPUR	10%	-16.39%	/	3,675.28%	/	182.58%	[47]
	30%	-52.88%	/	1,641.57%	/	3,077.67%	
PLA/silica	10%	92.68%	21.57%	/	/	/	[48]
PLA/Al	/	-16.56%	-1.71%	6.75%	/	/	[30]

Wood powder (or WF) is a suitable filler for improving the mechanical strength of PLA, however, owing to the poor compatibility between polar WF and the weakly polar PLA matrix [49], increasing the WF mass fraction deteriorates the mechanical properties of the FDM-derived composites. The WF-PLA interfacial compatibility can be improved by adding coupling agents such as KH550 or compatibilizers like maleic-anhydride-grafted polyolefin elastomer (POE-g-MAH) to enhance the mechanical properties of the composite, improving the processing fluidity and facilitating the FDMbased fabrication [50,51]. Luo and Sun [51] prepared PLA/ PBAT/poplar powder (WF) composites by melt blending with KH550 (a silane coupling agent), which enabled covalent PLA-PBAT coupling to form graft copolymers, thus improving the compatibility between the two phases. Yu et al. [6] improved the flowability of PLA/WF composite filaments by adding the acrylate resin (ACR) as a toughening agent, which increased the mechanical strength and $T_{\rm g}$ of the composite and diminished the water absorption. Du et al. [52] prepared maleic anhydride (MAH)/GMA-PLA compatibilizers by melt grafting and found that the tensile strength and impact strength of the WF/PLA composites increased by 9.54 and 7.23%, respectively, upon addition of the compatibilizers. Furthermore, the equilibrium torque, shear-generated heat, energy storage modulus, and complex viscosity of the composite system were

enhanced. Zhao *et al.* [53] prepared a GMA-*g*-PLA polymer capacitor through a melt reaction with dicumyl peroxide as an initiator; their strategy improved the interfacial compatibility between bamboo fiber and PLA and induced a significantly stronger capacitating effect than those by KH550 and MDI (4,4'-diphenylmethane diisocyanate).

Issues such as poor interfacial compatibility and warping can emerge when blending PLA with other polymers. To overcome these issues, Rasselet et al. [54] performed a twinscrew extrusion of PLA/polyamide 11 (PA11) melt blends using the multifunctional epoxide Joncryl as a solubilizer toward improving interfacial adhesion. The blends exhibited adequate ductility, improved tensile properties, and enhanced stiffness. Liu et al. [55] prepared PLA/PCL blends by melt blending with acetyl TBC (ATBC) as a bulking agent. With increasing ATBC content, PLA-PCL compatibility was improved and water absorption and tensile strength were reduced. The elongation at break and impact strength of the printed parts with 6% ATBC reached 94.6% and 10.5 kJ·m⁻², respectively. Geng et al. [56] prepared 3DP filaments by introducing ethylene/butyl acrylate/GMA terpolymer (PTW) into PC/PLA blends to alleviate warping. PTW reduced the shrinkage stress by hindering the crystallization of PLA to overcome the contortion and exhibited a notable toughening effect, enhancing the impact strength up to 46.3 kJ·m⁻². Yang et al. [57] used isosorbide diisocyanate (IBDI) as a bulking agent to prepare super-tough PLA/PCL blends by combining crystallization and reactive bulking, which improved the interfacial bonding strength between the poly(L-lactic acid) (PLLA) substrate and PCL. IBDI promoted the formation of stereocomplexation crystallization crystals (SC crystals) at the PLLA–PCL bonding interface and intensified the bulking effect. The notched impact strength and elongation at the break of the blend with 1.5 parts of IBDI were 68.4 kJ·m⁻² and 306%, respectively. Zhao *et al.* [58] prepared blends of PBAT, PLA, and an aluminate coupling agent (ACA) by melt blending. The ACA – which was used as a capacitating agent – was interspersed between the molecular chains of PBAT and PLA, which led to physical entanglement, improving the two-phase compatibility.

The percentage improvements in the mechanical properties of the aforementioned PLA composites with different additives are listed in Table 2.

3.1.3 Improvements in friction performance

Graphene improves wear resistance and reduces friction owing to its two-dimensional (2D) arrangement of sp²-bonded carbon atoms. Consequently, the addition of graphene to the PLA matrix yields a composite with excellent mechanical strength and retained flexibility, as well as customizable thermal and electrical conductivities, owing to the graphene network generated in the matrix. Bustillos *et al.* [59] developed PLA/graphene composites for 3DP, which exhibited a 14% improvement in wear resistance and a 65% reduction in the two-stage coefficient of friction in relation to those of PLA.

3.2 Improvement in porosity

Reducing the porosity of composite materials can moderately improve their mechanical properties [60]. For example,

Guessasma *et al.* [61] prepared PLA/PHA blends with low porosity (<6%) through FDM. Cardoso *et al.* [62] prepared PLA/PBAT blends using lower values of the printing parameters to produce parts with lower porosity, which improved their bending properties. Gurchetan *et al.* [63] prepared raw filaments as functional prototypes for 3DP using PLA/polyetherketoneketone/HAp-CS composites with 6.24% surface porosity, decent tensile properties (peak strength: 35.9 MPa; fracture strength: 32.3 MPa), a surface roughness of 42.67 nm, and a heat capacity of 2.14 J·g⁻¹. Kumar *et al.* [64] prepared PLA composites reinforced with polyvinyl chloride (PVC), wood chips, and magnetite (Fe₃O₄). The samples printed at the maximum density and a low filling angle exhibited minimum porosity and adequate mechanical properties (peak strength: 30.29 MPa; fracture strength: 25.58 MPa).

Graphene, HAp, and ceramic materials such as calcium phosphates - whose compositions are similar to that of the mineral phase of bone - are potential candidates for the manufacturing scaffolds used as bone substitutes and applicable in tissue engineering. Modification of PLA using these materials produces structures with increased porosity, allowing the application of such compounds in orthopedic scaffold construction and development of biomedical systems. Bakhshi et al. [65] prepared 3D porous PLA/Mg composite scaffolds by incorporating micrometer-sized Mg particles into the PLA matrix for FDM, with Mg improving the degradation rate and hydrophilicity of the PLA scaffolds. Milenkovic et al. [66] prepared novel, highly porous composites of PLA reinforced with lengthy, high-porosity polyvinylidene fluoride (PVDF) fibers. The composites exhibited significantly improved damage resistance, yield stress, and ductility owing to the PVDF fibers. Bustillos et al. [59] prepared highly porous PLA/graphene composites that exhibited higher hardness (146 MPa) and creep resistance (20.5% improvement) than those of PLA (123 MPa) despite their porous structure. Corcione et al. [67] synthesized HAp microspheres (sdHA) with a large specific surface area and enhanced cell adhesion by

Table 2: Mechanical properties of PLA composites incorporated with additives

Composite	Additive	Tensile strength	Elongation at break	Flexural strength	Impact strength	Ref.
PLA/WF	4% POE-g-MAH	36.88%	/	14.6%	30.21%	[50]
PLA/PBAT/WF	3% KH550	91.12%	90.16%	/	/	[51]
PLA/WF	ACR	13.83%	1	22.11%	35.17%	[6]
WF/PLA	2% MAH/GMA-PLA	9.54%	2.03%	3.82%	7.23%	[52]
BF/PLA	16% GPLA	72.1%	200.0%	118.1%	81.6%	[53]
PLA/PA11	3% Joncryl	/	308.3%	/	/	[54]
PLA/PCL	6% ATBC	/	84.6%	/	61.5%	[55]
PC/PLA	10% PTW	-11.15%	/	-16.18%	701.3%	[56]
PLA/PCL	2.14% IBDI	25.16%	705.26%	/	714.29%	[57]
PBAT/PLA	3% ACA	7.8%	43.84%	1	/	[58]

spray drying; these were dispersed in PLA by extrusion to obtain composite filaments, which were then used to fabricate sdHA/PLA scaffolds with high surface roughness and porosity. Nevado et al. [68] prepared 1.7-mm diameter PLA/ biphasic-calcium-phosphate composite filaments with HAp and tricalcium phosphate (TCP) acting as inorganic phases using a single-screw extruder. The composite exhibited high porosity for adequate cell proliferation and cell adhesion. Song et al. [69] used macadamia nut shells as a filler to modify PLA and employed the resulting composite filaments to prepare porous scaffolds with 30-65% porosity, 0.3-0.5 mm-sized connected pores, 0.1–1 um-sized micropores, and 37.92-244.46 MPa elastic modulus for FDM-based fabrication of lightweight structural components.

3.3 Improvements in thermal performance

The thermal stability of PLA is comparable to that of PVC but lower than that of polymers such as PP, PE, and PS. The PLA processing temperature is generally controlled to 170-230°C, which is suitable for processes including injection molding, stretching, extrusion, blow molding, and 3DP. However, the crystallization rate and crystallinity of PLA are low during processing, resulting in a low heat deflection temperature, which limits its applications in the hot filling or heat sterilization processes of product packaging. Consequently, PLA requires modifications.

To enhance the crystallization rate and crystallinity of PLA, the optical purity of PLA should be increased as much as possible during production. Annealing or the addition of nucleating agents can improve the crystallization behavior, consequently increasing the heat deflection temperature and heat resistance. Zhang et al. [30] prepared Al/PLA composite specimens for FDM and found that the energy storage modulus and T_g of the composites were higher than those of PLA; thus, adding Al fibers could improve the heat resistance of PLA. Xue et al. [70] added 2 wt% ammonium polyphosphate (APP) and a 0.12 wt% resorcinol bis(diphenyl phosphate) (RDP) solubilizer to PLA. RDP improved the dispersion of APP particles in PLA, enhancing the flame retardancy. The 3D-printed products of the PLA/APP/RDP composites exhibited mechanical properties comparable to those of pure PLA along with adequate flame retardancy. Zerankeshi et al. [71] prepared PLA/graphite composites by partially dissolving the surface of PLA particles with dichloromethane, which produced a cohesive surface that enhanced the adhesion of the powder. The composites exhibited higher $T_{\rm g}$ and crystallinity than those of PLA, indicating improvements in the thermomechanical properties. Vardhan et al. [72]

proposed spraying Al and PLA alternatively to manufacture composites with higher tensile strength and thermal conductivity than those of pristine PLA for FDM, which could be exploited to dissipate heat in electronic devices.

4 Functionalization of PLA composites for 3DP

3DP technology allows easy and accurate fabrication of functional materials that can be used in various fields. Additives selected for specific applications are blended with PLA matrix polymers for functional composite modification, which can be used in biomedical, engineering applications, conductivity, electromagnetism, sensors, and other industries [73].

4.1 Shape-memory function

When a shape-memory polymer (SMP) is subjected to an appropriate stimulus, its internal structure rearranges and can change from a programmed temporary shape to an original permanent shape. Stimuli can be provided in the form of heat, light, electricity, moisture, pH, or magnetic field. SMPs have been used to develop new smart materials owing to their moderate cost, low density, and potential biocompatibility and biodegradability. Common SMPs such as PU, poly(ethylene vinyl acetate), and PCL can be compounded with PLA to impart the shape-memory functionality to FDM-based 3D-printed products.

Liu et al. [74] prepared SiC/C/PLA composite filaments for FDM-based 3DP of parts with thermally responsive shape recovery properties. To that end, the thermal conductivity and, consequently, the shape-memory responsiveness were controlled using material ratios, which reduced the recovery time by 87% in relation to that of pure PLA. The shape-memory behavior of pure PLA with an SiC fiber filament and that with a graphite-containing filament was observed (Figure 6a and b). Wang et al. [75] prepared PCL/ PLA blends whose toughness increased with increasing PCL content and whose shape-memory recovery rate reached up to 95.37%; Figure 6c shows the thermally activated shapememory behavior of PCL/PLA with different PCL/PLA ratios. Hua et al. [76] fabricated flexible photo-responsive shapechanging actuators through FDM-based 3DP using PLA/ MWCNT composites. MWCNTs exhibit excellent photomechanical properties that can improve the processability and photosensitivity of PLA; for example, 3D-printed brakes 10 — Yishan Li et al. DE GRUYTER

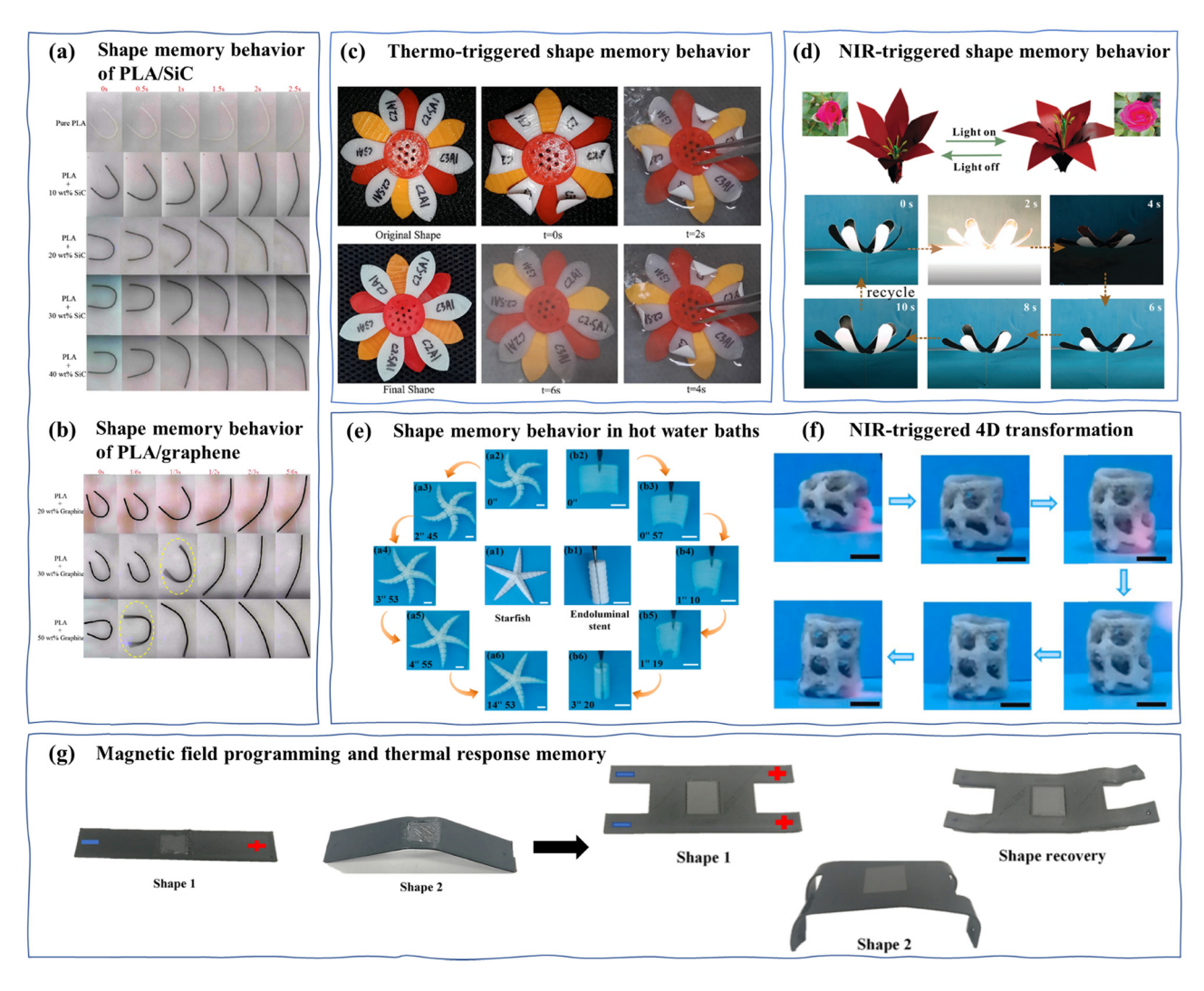


Figure 6: Sequential images showing the shape recovery of pure PLA and (a) SiC-filament-containing and (b) graphite-filament-containing PLA [74]. (c) Thermally activated shape-memory behavior of PCL3/PLA1, PCL2.5/PLA1, and PCL2/PLA1 [75]. (d) Schematics and photographs of flowers in the closed and blooming states, and phototriggered shape-changing behavior of a 3D-printed flower that blooms like a flower from closed to open states [76]. (e) Shape-memory behavior of 4D-printed PBS/PLA architectures: (a1–a6) starfish and (b1–b6) endoluminal stent; (a1, b1) permanent and (a2, b2) temporary configurations; and (a2–a6, b2–b6) shape recovery processes. (f) Dynamic, remote, and precisely controlled 4D transformation of a GO-functionalized porous PBS/PLA scaffold actuated by an NIR laser at a power density of 5 W·cm⁻² [77]; (g) A 1D beam shape was transformed to a 2D shape using a permanent magnet and 60 V power supply, and a 2D rectangular shape was converted to a 3D structure with 93% shape recovery through Joule heating after magnetic remote programming [78].

can sense and act in a predetermined order upon near-infrared (NIR) irradiation (Figure 6d). Lin et al. [77] prepared PBS/PLA composite filaments with shape-memory characteristics for four-dimensional (4D) printing, and the functionalized PBS/PLA porous scaffold exhibited NIR-triggered shape-memory behavior (Figure 6e, f). The aforementioned composites have promising applications in the biological field – particularly in interventional procedures – and can achieve dynamic, accurate, and remotely controlled 4D temporal transitions. Dezaki and Bodaghi [78] prepared ironfilled magnetic PLA and carbon black (CB)-filled conductive PLA composites and then used them to construct 4D-printed

actuators. The devices recovered rapidly to their previous shape when powered by a 120 V power supply. Additionally, a maximum bending angle of 59° was attained under an external low-intensity magnetic field (Figure 6g).

4.2 Biocompatibility and osteoconductive properties

PLA is biodegradable and has good prospects in biomedical applications such as printing scaffolds through FDM [79].

However, PLA has disadvantages such as low osteoconductivity, acidic degradation, and insufficient surface cell adhesion, which limit its tissue engineering applications. To overcome these limitations, PLA mixtures have been modified using additives or biocompatible materials, thereby conferring excellent osteoconductive properties and biocompatibility to 3D-printed products. Furthermore, a lowtemperature coating can be applied onto the surface of 3D-printed PLA products to impart biocompatibility and antibacterial ability to the scaffolds.

Owing to its decent biodegradability, biocompatibility, cell proliferation ability, and nontoxicity, PLA is extensively used as a biodegradable medical material for tissue engineering and drug delivery applications. Guerra et al. [80] prepared PLA/PCL composite scaffolds at an average cell proliferation rate of 12.46% after 3 days through FDMbased 3DP. Mystiridou et al. [81] used PLA/PCL as the matrix and HAp and barium titanate (BaTiO₃) as fillers, which significantly enhanced the dielectric properties and yielded piezoelectric coefficients close to those of the human bone. Najera et al. [82] added a small amount of TiO2 to PLA/ PCL composites, whose 3D-printed parts exhibited excellent in vitro biocompatibility and properties similar to those of cancellous bone.

In addition to PCL, HAp – which is the main inorganic component of human and animal bones - can form chemical bonds with body tissues at interfaces. Moreover, HAp has a certain level of solubility in the body, releasing ions that are harmless to the body, participating in body metabolism, and exhibiting a stimulating and inducing effect on osteophytes [83,84]. Fan et al. [85] modified PLA with PEG and HAp and then 3D-printed a porous scaffold surface suitable for cell adhesion, growth, and differentiation; the porous scaffold and cells stabilized after 12 h. Wang et al. [86,87] prepared a PLA/nano-HAp composite branch that provided a suitable environment for cell adhesion and growth and had the ability to osteoconduct and guide bone regeneration. However, the mechanical properties deteriorated with increasing n-HAp content (Figure 7e, f). Microcomputed tomography (micro-CT) of the implanted scaffolds (Figure 7a) showed defects in the surgical area of the PLA group, but not in the composite group three months after surgery. 3D reconstruction of the cortical area of the implanted scaffold (Figure 7b) indicated that the PLA group was porous and had surface vacancies, while the composite group had a dense outer layer of the new bone. Regardless of the filling rate of the new bone or total stent density, the n-HAp-containing groups exhibited significantly higher values than those of the PLA groups (Figure 7c and d).

Calcium phosphate is another major inorganic component of bone tissues, which can form chemical bonds with living tissues and exhibit excellent osteoconductivity. Donate et al. [13] used calcium carbonate and B-TCP as additives in PLA-based support structures to increase the degradation rate of 3D-printed scaffolds. Salamanca et al. [88] prepared a PLA/β-TCP hybrid for guided bone regeneration and discovered that using 10% B-TCP with PLA in FDM-based 3DP was more effective than using pristine PLA, leading to enhanced cell proliferation and osteogenic differentiation. Jiang et al. [89] prepared hydroxypropyl methylcellulose/PLA composite filaments containing 7% hydroxypropyl methylcellulose, which significantly enhanced the hydrophilicity of the composite, reduced the water contact angle by 30°, resulted in a lower crystallinity (3.7%) than that of pure PLA (4.5%), and improved the degradation rate of the polymer. Kohan et al. [90] prepared PLA/PHB + HAp/TCP composite filaments and successfully printed intervertebral disc implants. Yang et al. [91] prepared a crab-shellpowder/PLA composite using waste crab shells and PLA. The PLA-1.5ESCSP composite exhibited high antibacterial activity (>99%) against Escherichia coli and decent biocompatibility.

To avoid the high-temperature effect of FDM-based 3DP on fillers such as temperature-sensitive drugs, bioactive molecules, and temperature-variable biomaterials, PLA has also been imparted with bioactivity through coating or embedding. Kamath et al. [92] embedded PCL scaffolds into FDM-fabricated 3D porous PLA scaffolds; they also prepared composite scaffolds containing n-HAp and MWCNTs to improve mechanical strength while introducing bioactive molecules, confirming the osteoconductivity of the scaffolds. Lett et al. [93] prepared a low-temperature coating by compounding polyvinyl alcohol and Ag-HAp and applied it to a PLA stent. In vitro hemocompatibility tests of Ag-HAp/PLA indicated that the complex exhibited less than 2% hemolytic activity and decent compatibility with human blood. Reina et al. [94] modified the surface of PLA scaffolds using an HAp/gelatin coating, which improved the bioactivity and hydrophilicity of PLA. The notable biocompatibility and cellproliferation-enabling tendency of gelatin could be leveraged to construct mandibular reconstruction scaffolds.

4.3 Biodegradability

Biodegradable materials include biodegradable alloys and biodegradable plastics. Biodegradable alloy materials have high strength, low density, and elastic modulus close to human bone. They are prone to corrosion and destruction in physiological environments until they completely disappear, and their degradation products can be metabolized and absorbed by the human body. As implant materials, they can avoid secondary surgery [95,96]. Biodegradable

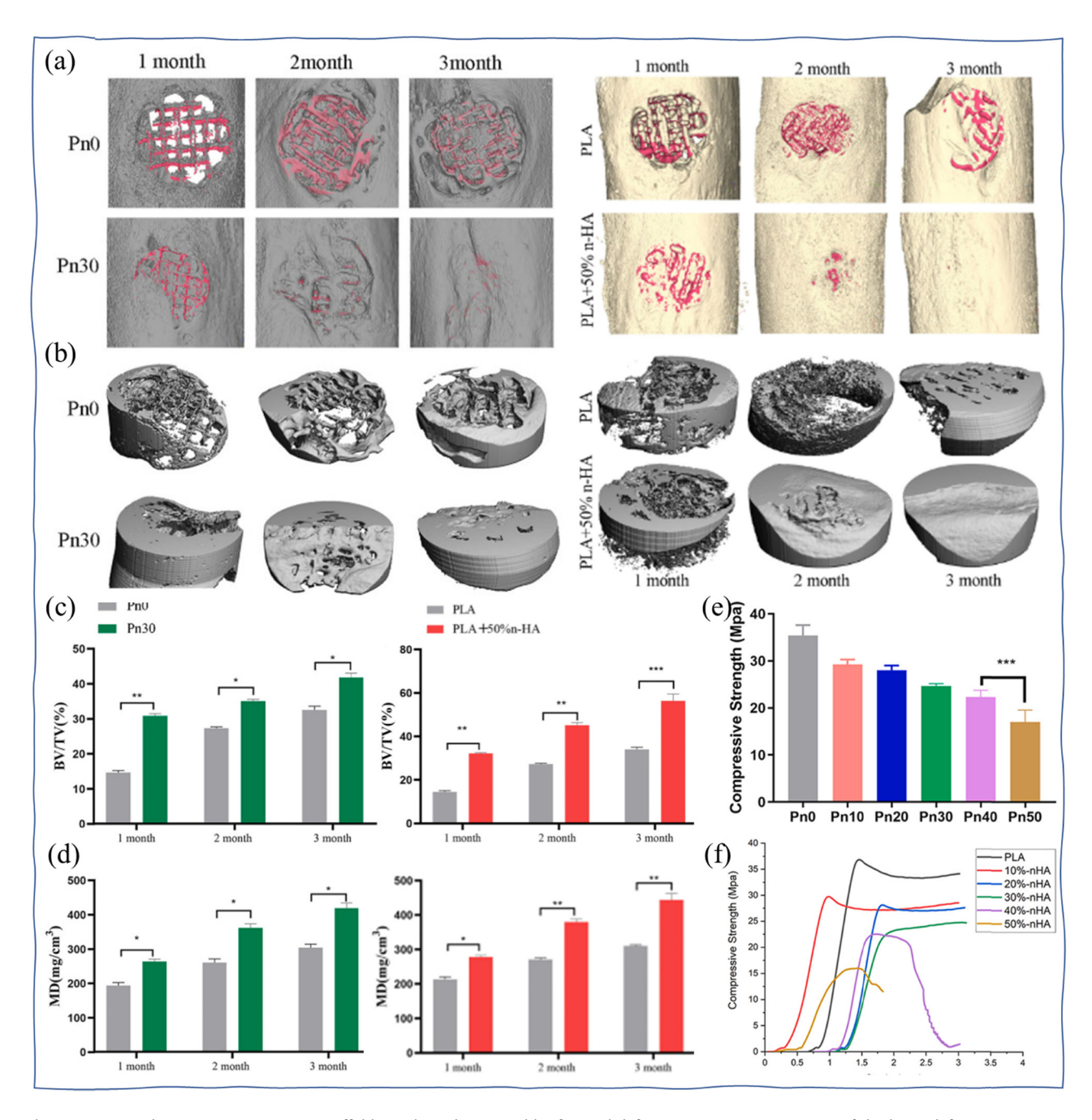


Figure 7: PLA and PLA/n-HAp composite scaffolds implanted into a rabbit femoral defect. (a) 3D micro-CT images of the bone defect center were acquired 1, 2, and 3 months after implantation of the 30% n-HAp stent (diameter, 5 mm); the stent is shown in red. (b) 3D images of new bone formation in Pn0 and Pn30 implants reconstructed through micro-CT. (c) Bone tissue volume/total tissue volume (n = 3). (d) Mineral density (MD; n = 3). *p < 0.05; **p < 0.01. (e, f) Pressure test results (n = 4; ***p < 0.01) [86,87].

plastics typically comprise biodegradable/bio-derived polymeric matrices with natural organic fibers/particles (as fillers or reinforcements). In recent years, the environmental problems caused by plastic waste and the high cost of bioplastic development have stimulated research on green composites to satisfy the demand for sustainable materials from multiple economic and ecological perspectives.

Scaffaro *et al.* [97] used two different natural fillers from marine and agricultural wastes – *Posidonia oceanica* leaves and *Opuntia ficus-indica* cladodes – to prepare powders for incorporation into PLA matrices for FDM-based 3DP. The results indicated that up to 20% of bioplastics could be replaced with alternatives having the aforementioned low-cost, environmentally friendly natural fillers without

significantly altering the processability and mechanical properties of the pure polymer. Moreover, the biocomposites were more hydrophilic than pure PLA, which improved their biodegradability/compostability. Ertane et al. [98] used biochar – prepared by pyrolyzing wheat stems – to reinforce PLA, yielding a biodegradable composite that could be used as a structural material for soil amendment at the end of its useful life. Hanumantharaju et al. [99] prepared 3D printable biocomposites from eggshell (ES)-powder-reinforced PLA and performed biodegradability tests. These tests showed that PLA/ES10 exhibited the highest biodegradability among the samples and could be used as a bioresorbable material for biomedical applications. Li et al. [7] produced a novel TOBC material to reinforce PLA, which facilitated the formation of a 3D-networked, crosslinked, and fully biodegradable composite for FDM. Salehi et al. [100] prepared PLA/PEG composites that are applicable in bone tissue engineering. The use of 20 wt% PEG decreased the water contact angle from 78.16° to 60.00°, enhanced the hydrophilicity, and increased the degradation rate to 50.96%.

4.4 Moisture absorption

Moisture absorption is an indicator of the physical properties of fibers, with materials having multiple capillaries exhibiting higher moisture absorption capacities. The moisture absorption performance of PLA-based 3D-printed materials has been improved by compounding fibrous or porous materials with PLA. However, the hydrophobicity of PLA and the hydrophilicity of natural fibers lead to weak interfacial bonding among the 3D-printed components, which negatively affects their mechanical properties. Quader et al. [101] prepared PLA/PBS filaments with different ratios and demonstrated the effects of hygroscopicity on the mechanical properties, and those of the PBS content on interfacial compatibility.

Kariz et al. [102] prepared 3D-printed filaments using WF and PLA. Specimens fabricated using filaments with higher WF contents had higher moisture contents, larger dimensional expansion, and lower modulus of elasticity, which facilitated the formation of 4D-printed materials for designing products with climate-dependent attributes. Tomec et al. [103] exploited the anisotropic expansion properties of natural fibers in wood to prepare PLA-based biocomposites by compounding. These biocomposites were used to develop bilayer actuators with moisture-induced deformation, in which wood caused dimensional changes owing to water adsorption and desorption. FDM-printed materials prepared by exploiting this shape change could

be applied as ventilation valves for climate moisture monitoring and control.

4.5 Absorbency

Although the PLA resin is not inherently adsorptive, it forms a network structure when compounded with a material having highly adsorbing components. This can confer adsorptive characteristics to PLA, thus broadening the application scope of PLA materials, particularly those prepared through 3DP, and enhancing the applicability of 3D-printed materials as adsorbents. Zheng et al. [104] melt-blended PLA with PBS as the base resin and camellia seed powder after degreasing camellia seeds. Subsequently, products were obtained through FDM-based 3DP. Analysis of the water contaminant removal capacity indicated that when the camellia seed powder content of PLA/PBS reached 30 phr, the composite transformed from "liquid-like" to "solid-like" states and formed a network structure with an adsorption rate of 85.33%.

4.6 Electrical conductivity and electrical heating properties

PLA can be used as a base material to prepare electrically and thermally conductive composites by using conductive fillers such as CB [105-107], graphene [108-111], carbon nanotubes (CNTs) [112-114], and carbon nanofibers (CNFs) [115-117]. These polymer composites are widely used in systems including antistatic plastics, electromagnetic-shielding substances, self-temperature control heating materials, positive temperature coefficient materials, and environmentally sensitive devices. PLA-based conductive polymer composites which are typically degradable and biocompatible – can be used to develop systems including special antistatic packaging, electromagnetic-shielding packaging, smart packaging, and gas/liquid sensors for food quality detection.

Sathies et al. [105] synthesized 3D-printable PLA/CB sensors suitable for solvent sensing. Stefano et al. [107] prepared CB/PLA composite filaments by adding 28.5% CB to PLA. These filaments were applied as electrochemical sensors upon FDM-based 3DP and their ability to detect catechol and hydroguinone in water samples and hydrogen peroxide in milk was assessed. Tirado-Garcia et al. [106] 3Dprinted PLA/CB polymers and found that the magnitude and direction of mechanical deformation affected the extent of the resistance or current. Daniel et al. [108] found that

3D-printed PLA/graphene- and PLA/CB-based components exhibited up to 1,500 and 300 times higher resistivities than that of a single extruded wire. Tan et al. [109] fabricated simple resistance temperature detectors through FDM-based 3DP using two types of conductive PLA filaments - incorporated with CB and graphene - exhibiting conductivities of 0.0238 and 0.1042 mS for CB/PLA and graphene/PLA sensors, respectively. The fabricated systems were used as temperature sensors and exhibited decent flexibility and stability even after being transferred to different substrates. Kim and Lee [110] prepared graphene/PLA filaments and 3D printed differently shaped electrical heating elements on cotton fabric through conveyor FDM. These heating elements showed enhanced resistivity and electrical heating properties of samples and excellent electrical heating performance over an extended period [111].

Ye et al. [118] prepared graphene/FeSiAl/PLA composites with different amounts of graphene, which exhibited significantly improved electromagnetic wave absorption properties. Moreover, the distance between conducting particles decreased and the conductivity loss increased with increasing graphene content. Folds and holes appeared in these graphene-loaded composites, forming a graded structure that facilitated multiple reflections and scattering of electromagnetic waves, and enhanced the interfacial polarization loss. Amirov et al. [119] prepared PLA composite filaments containing ferrite, and 3D-printed magnetic parts with specific magnetization strengths to create magnetically controlled gears, actuators, and robotic components. Ye et al. [120] prepared FeSiAl/PLA and FeSiAl-MoS2-graphene/ PLA composite filaments through mechanical mixing to 3D print wave-absorbing bilayer materials via FDM. FeSiAl-MoS₂-graphene/PLA exhibited good impedance, matching with that of air. A double-layer absorber with FeSiAl/PLA and FeSiAl-MoS₂-graphene/PLA as the first and second layers, respectively, exhibited a low reflection loss and had a small thickness and wide effective absorption bandwidth (EAB). The $R_{\rm L,min}$ value was -52.50 dB at 17.76 GHz when the two layers were 0.6 and 1.1 mm thick, respectively. Moreover, the EAB value of the double-layer absorber was 5.92 GHz (12.08-18 GHz) for a total thickness of 2.0 mm, which was 29.8% wider than that of the FeSiAl-MoS2-graphene/PLA composite with the same thickness. Additionally, composite microspheres with reduced graphene oxide (rGO) and carbonyl iron powder (CIP) were prepared by solvent volatilization. The effective combination of rGO and CIP in the composite microspheres helped achieve synergy in terms of multiple loss mechanisms and adequate electromagnetic absorption. The absorbing performance of the rGO-CIP/PLA composite filaments improved and then deteriorated with increasing rGO addition, with optimal absorbing

performance achieved by the rGO-CIP/PLA-4 composite with 5.1 wt% rGO. The maximum reflection loss (-50.1 dB) and the maximum EAB (6.24 GHz) were achieved at material thicknesses of 2.2 and 2.0 mm, respectively [121]. Yang *et al.* [122] produced CNT/PLA composite films with excellent electromagnetic interference shielding and electrothermal properties by FDM; among these, 4 mm-thick 4 wt% CNT/PLA films achieved an electromagnetic interference shielding of 68 dB at 12.3 GHz. Wang *et al.* [123] coated highly conductive CNT on 3D-printed PLA scaffolds and achieved composite EMI shielding values of up to 67 dB when 5.0 wt% CNT was added, which can be used in different radiation source fields and electronic devices.

5 Compositing-based modification of PLA using nanomaterials

PLA nanocomposites have excellent properties owing to the small size, high specific surface area, and strong interfacial binding attribute of nanoparticles. Table 3 summarizes the characteristics of PLA composites with different nanomaterials.

5.1 Carbon-based nanomaterials

These nanomaterials include carbon-based substances as a dispersed phase with at least one dimension less than 100 nm. The dispersed phase typically comprises carbon atoms, heterogeneous (noncarbon) atoms, or even nanopores. Carbon nanomaterials are generally categorized into CNTs, CNFs, and carbon nanospheres (CNSs). Nanocarbon/PLA composites embedded with MWCNTs and graphene nanoplates (GNPs) for 3DP have been found to achieve a low permeation threshold, high electrical conductivity, and high thermal conductivity [112,124,125]. Moreover, the incorporation of carbon nanostructures with predominantly 2D shapes (GNPs) into the PLA matrix has led to superior thermal conductivity. DC measurements showed that the nanocomposites filled with 1D carbon nanoparticles (CNTs) and 2D fillers (GNPs) exhibited a low electropermeability threshold and higher postpermeability conductivity, respectively [113]. PLA composites 3D-printed with carbon nanomaterial fillers can be considered excellent electrical and thermal conductors for various applications.

5.1.1 CNTs

CNTs are seamless, hollow, small-diameter tubes formed by coiling graphene sheets having carbon atoms, with the

 Table 3:
 Characteristics of PLA/nanomaterial composites

Nanomaterial	Characteristic features	Attributes of its composites with PLA	Functionalities	Applications
Carbon	High specific surface area	As filler: improves the electrical and thermal properties	Mimics the extracellular matrix; enhances the cell adhesion, differentiation, and proliferation; enables conductivity	Biomedical materials, electrothermal applications, multifunctional filaments, conductive composites
	High thermal conductivity	One-dimensional (1D) carbon nanomaterials (e.g., CNTs) have a low electro-permeation threshold	`	
	High electrical conductivity	2D carbon nanomaterials (e.g., graphene nanoplates; GNPs) have higher postpercolation conductivity		
	High chemical inertness Low density			
Nanocellulose	High specific surface area	As filler: improved mechanical properties and biodegradability	Acts as a nucleating agent and enhances interfacial compatibility	Enhanced printability, sensing technology
	High crystallinity Good hydrophilicity High transparency Good biodegradability and	Improved crystallinity Increase tensile modulus, tensile strength Improved biodegradability		
	biocompatibility Stable chemical properties			
Nanosilver	Electrical conductivity Surface effects Ouantum size effects	Superior thermal properties	Antibacterial properties	Biomedical devices, antimicrobial surgical devices, composites for thermal sterilization
Nanocopper	Superplasticity Ductility	Increased bending strength Increased compressive strength	Antibacterial properties	
Nanoclay	Thermal stability	Reduced crystallinity	Osteogenic properties, biocompatibility, ability to operate as a nucleating agent	Biomedical
	Dimensional stability Excellent barrier properties Antistatic and flame retardant properties Dimensional stability	Increased modulus of elasticity		
Nano-HAp	High surface area	Improved thermal stability	Biocompatible and osteogenic induction, highly printable, mimics the inorganic phase of natural bone	Repair of large bone defects
	Strong chemical activity High void ratio, negative charge	Increased modulus of elasticity Suitable compressive strength		
Nanosilica	Anti-ultraviolet optical properties Small size, surface, and macroscopic quantum tunneling effects	Good hygroscopicity Improved tensile strength Increased bending modulus	Hydrophobic, excellent moisture resistance	Hydrophobic coatings, liquid level control

outer diameter of the tube generally ranging from a few to tens of nanometers and an even smaller inner diameter (e.g., ~1 nm). The addition of CNTs affects the fluidity, crystallization, and melting behavior of PLA and improves its mechanical strength [126] and electrical conductivity. Yang et al. [127] prepared PLA/CNT composite filaments for FDM, which exhibited 64.12 and 29.29% higher tensile and bending strengths, respectively, than those of pure PLA. Rebaioli et al. [128] used 3 wt% CNTs to prepare 3D-printed composite scaffolds with higher specific electrical conductivity than that of pure PLA, superior matching with the host bone, and enhanced cell adhesion, differentiation, and proliferation. Mohapatra et al. [129] 3D-printed a frictional triboelectric nanogenerator using PLA and acrylonitrile butadiene styrene as the frictional positive and frictional negative layers, respectively. Moreover, they reinforced PLA with CNT/ZnO core-shell structures (CNSs) to improve its mechanical strength and charge generation capability (Figure 8), resulting in an output voltage of up to 8.9 V and an increase in conductivity by five orders of magnitude.

The surface of MWCNTs is considerably more active than that of single-walled CNTs owing to surface groups such as carboxyls. MWCNTs can play the role of crystal nuclei; promote crystallization; lower the $T_{\rm c}$, $T_{\rm g}$, and $T_{\rm m}$ of the composite; and improve the shielding effect of the material against electromagnetic waves and electrical conduction. Moreover, PLA/MWCNT composites are generally amenable to FDM [130]. Luo *et al.* [114] prepared conductive PLA/MWCNT composites for 3DP. The conductivity of pure PLA after 3DP was $1.06 \times 10^{-15} \, \mathrm{S \cdot cm^{-1}}$, which classifies

it as an insulating material, while that of the composite containing 5% MWCNTs was $0.4 \pm 0.2\,\mathrm{S\cdot cm^{-1}}$. Kamath *et al.* [92] embedded MWCNTs into a PLA/PCL matrix to improve biocompatibility and osteoconductivity, providing a novel 3DP approach for developing biomedical scaffolds. Cobos *et al.* [131] used maleated linseed oil as a lubricant to prepare PLA/MWCNT and PLA/halloysite-nanotube composites with improved rheological properties. The crystallization temperature and flowability of the obtained composites were ~12°C lower and ~47% higher, respectively, than those of pure PLA. Lage-Rivera *et al.* [132] developed PLA/MWCNT filaments with good electrical properties and suitable processability using lignin as a plasticizer, which strengthened the conductive network and increased the electrical conductivity by six orders of magnitude.

5.1.2 Graphene nanosheets

GNPs are ultrathin-graphene-based layered stacks that have more than 10 carbon layers and thicknesses of 5–100 nm. GNPs maintain the original planar, carbon hexa-ring, conjugated crystal structure of graphite, and exhibit decent lubrication, high temperatures, and corrosion resistances. They are typically used as fillers to modify PLA because they impart excellent mechanical strength, as well as electrical and thermal conductivities. Combining rGO, MWCNTs, and graphite can produce composites with further improved electrical and thermal conductivities. For instance, combining rGO and graphite reduced the resistivity by an order of

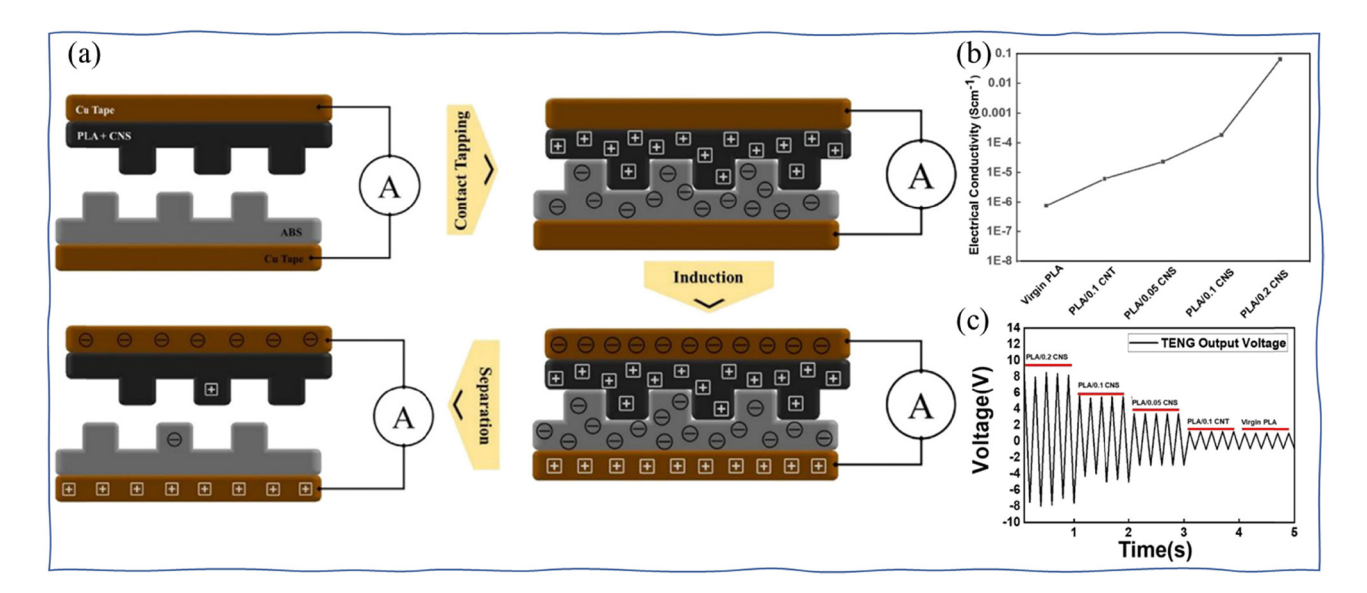


Figure 8: (a) Working mechanism of a triboelectric nanogenerator comprising PLA, CNSs, and ABS as the triboelectric layers. (b) Electrical conductivity and (c) triboelectric nanogenerator output voltage for PLA and PLA/CNS nanocomposites [129].

magnitude and increased the thermal conductivity by 25.71% [133]. Kim et al. [134] prepared a GNP/PLA composite with a 44% increase in tensile strength and electrical conductivity over 1 mS·cm⁻¹. Vidakis et al. [135] compared the mechanical response and electrical conductivity of FDM-derived specimens of pure PLA and PLA/GNP. The poor solubility and compatibility of the GNPs with respect to PLA led to the PLA/GNP composites exhibiting a slightly inferior performance to that of PLA; however, the dielectric constant of the composites (4.50) was significantly higher than that of PLA (3.45). Suitable modifiers can be employed to improve the solubility and compatibility of GNPs with respect to PLA. Wang et al. [136] used 2 wt% L-arginine as a modifier for PLA/ GNP composites, increasing the tensile and flexural strengths by 43.6 and 28.5%, respectively.

5.1.3 CNFs

CNFs are fibrous carbon nanomaterials made from multilayered graphite flakes curled together with a high degree of crystalline orientation. These nanomaterials have good electrical and thermal conductivities. Maynard et al. [117] dry-blended PLA with CNFs, processed them in a singlescrew extruder, and printed products using FDM. These products were then used to prepare piezoresistive sensors, actuators, and electrical components. The prepared 5 wt% CNF/PLA composites showed a reduction in resistivity of up to 16 orders of magnitude compared to that of unmodified PLA. Hernandez et al. [116] added 7.5 wt% CNFs into granular PLA for dry blending, and the product was subjected to multiple recovery/re-extrusion cycles in a singlescrew filament extruder, resulting in the CNFs forming a conductive network within the PLA. The 10.0 wt% CNF/PLA sensor showed greater repeatability in its piezoresistive response and the effect of sensor size on strain sensing performance was lower than those of the 7.5 wt% CNF/ PLA composite. The 10.0 wt% CNF/PLA sensor was used to fabricate strain sensors by additive manufacturing [115].

5.2 Nanocellulose

Cellulose nanocrystals (CNCs) and cellulose nanofibers are naturally occurring nanofillers that can reinforce PLA to improve its mechanical and biodegradable properties. Kumar et al. [137] 3D-printed PLA/CNC composites that exhibited a 50% higher tensile modulus and 18% higher tensile strength than those of pure PLA. Zhang et al. [138] reinforced PLA using lignocellulosic CNFs, whose internal lignin component operated as a binder to improve the interfacial compatibility of the composites. The composites with 3.7% lignin exhibited a 153% higher flexural strength than that of pure PLA.

Micro-nanocellulose (MNC) - the most abundant natural polymer carbohydrate – has the advantages of being light weight and having high strength, a high specific surface area, and a low thermal expansion coefficient. It is widely used to manufacture products such as paper, food, and electronic equipment. However, PLA/MNC composites typically exhibit subpar interfacial compatibility, which can be boosted by using the silane coupling agent KH550 [139]. For instance, Wang et al. [140] developed an MNC/PLA 3DP filament modified with 30 wt% KH550 to improve the interfacial MNC-PLA compatibility. This was then compounded with PEG6000 and PLA to yield a product that had an elongation at a break of 12%, a tensile strength of 59.7 MPa, and a flexural strength of 50.7 MPa.

5.3 Nanometals

Nanosilver particles exhibit an intense sterilization effect and have ultrahigh permeability; the smaller the particle size, the stronger the bactericidal properties. Maroti et al. [141] prepared PLA/Ag nanocomposite filaments for 3DP biomedical devices. Nanosilver can promote wound healing, accelerate the repair and regeneration of damaged cells, exhibit antibacterial and anti-inflammatory properties, improve the microcirculation of the tissues around wounds, effectively activate and promote tissue cell growth, and reduce scar generation. Bayraktar et al. [142] prepared silver nanowireloaded PLA nanocomposites which were then 3D printed to obtain the desired shapes, 4 wt% of silver-loaded nanocomposites were able to kill 100% of E. coli and Staphylococcus aureus in 2 h and sustained E. coli killing in 24 h and S. aureus killing in 8 h. Tzounis et al. [143] synthesized PLA/Ag composites to prepare Army/Navy retractors with antimicrobial activity and on-demand geometry using FDM-based 3DP; the composites were 10 times less expensive than their stainless steel counterparts. Figure 9a and b shows TEM images of an ultrathin film section of the PLA/Ag retractor. The Ag layers comprising AgNPs exhibited polycrystalline properties typical of nanoparticle-based films. The AgNPs were adequately distributed along the PLA surface and penetrated PLA, resulting in good adhesion at the interface, and the release of Ag ions without separation of the AgNP films. Antibacterial activity experiments indicated that the bacterial culture was eradicated after 120 min (Figure 9c). Ekonomou et al. [144] developed antimicrobial FDM-based 3DP materials made of Cu/AgNP-loaded PLA and TPU, which exhibited

18 — Yishan Li et al. DE GRUYTER

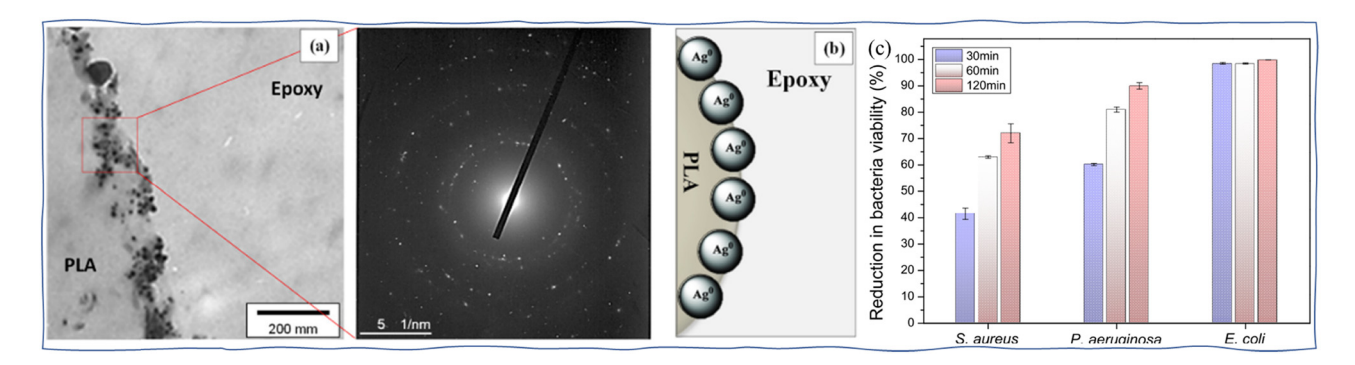


Figure 9: (a) TEM image of the PLA/Ag retractor cross-section and the corresponding SAED pattern showing the nanoscale characteristics of the AgNP layer. (b) Illustration of the main finding from the TEM cryosection analysis, describing the "penetration" of the AgNPs into the outer surface of PLA (by a few nanometers). (c) Antibacterial activity of PLA/Ag toward *E. coli, P. aeruginosa*, and *S. aureus* after 30, 60, and 120 min of contact [143].

decent hydrophobicity compared to that of ordinary polymers, and showed potential as antimicrobial materials in biomedical and food-related applications. Copper nanoparticles can elongate more than 50 times at room temperature without cracking. Leveraging this fact, Balamurugan *et al.* [145] prepared 14 wt% PLA/Cu composites with excellent compressive and flexural strengths for FDM, which induced decent bonding between copper and PLA.

5.4 Nanoclay

Nanoclay can function as a nucleating agent and improve the elastic modulus of 3D-printed samples. Coppola *et al.* [10,11] prepared PLA/clay nanocomposites in which a layered silicate (Cloisite 30B) and nanoclay improved the crystallinity and thermal stability of PLA, respectively. The 3D-printed nanocomposites exhibited a higher elastic modulus (15%) and superior shape stability than those of pure PLA [146].

5.5 Nano-hydroxyapatite

HAp – which is the crystalline part of natural bone – is nontoxic, harmless, bioactive, and osteoconductive. However, the brittleness and low fatigue strength of pristine HAp in physiological environments limit its application in bone repair or bone replacement under load; therefore, it is not optimal as a bone-tissue-recovering or structural material. Nevertheless, the combination of PLA and HAp has recently been found to improve the overall performance of HAp while providing medical material suitable biocompatibility [92]. Compounding high-elastic modulus HAp with PLA can improve the mechanical properties and

biocompatibility of HAp, particularly for hard tissue repair materials.

Wang *et al.* [86,87] prepared PLA/n-HAp composite scaffolds using FDM and tested osteogenic induction *in vitro*. The composite scaffolds exhibited sufficient mechanical strength, suitable pore size, biocompatibility, and an osteogenic induction performance that was significantly superior to that of pure PLA scaffolds. Zhang *et al.* [147] prepared porous PLLA/n-HAp bone repair scaffolds by FDM using PLLA (L-PLA)/n-HAp composites. The composite scaffolds had significantly higher compressive strengths than those of human cancellous bone and Ca–P porous ceramics, with the specimens having high n-HAp loading exhibiting superior *in vivo* bone regeneration ability.

5.6 Nanosilica

Nanosilica is an amorphous white powder with molecules arranged as 3D chains, reticular structures, or silica configurations. The introduction of nano-SiO₂ into polymers to prepare nanocomposites has attracted considerable interest because of the resulting improvements in the modulus, strength, and thermal stability of polymers. However, nanosilica – whose surface is rich in hydrophilic silicone hydroxyl groups - cannot be readily dispersed uniformly in the polymer because of its poor compatibility with organic materials. Consequently, silane coupling agents are generally used to eliminate or reduce the content of the surface silicone hydroxyl groups to improve hydrophobicity. Subsequently, the compatibility between nanosilica and monomers/polymers improves and nanocomposites can be produced by in situ polymerization and blending. Seng et al. [148] demonstrated that adding 1% treated nanosilica as a filler reduced the hygroscopicity of 3D-printed filaments by 40% and improved its tensile properties compared to those of PLA. Ramachandran and Rajeswari [149] prepared PLA/nanosilica filaments by coblended extrusion and obtained 3D-printed products with the highest hardness and tensile, compression, flexural, and impact strength among the specimens using a low coefficient of friction and a specific wear rate. Lee *et al.* [150] coated hydrophobic SiO₂ nanoparticles and methyl ethyl ketone onto 3D-printed PLA parts by dip coating to fabricate superhydrophobic surfaces.

6 3DP applications of PLA composite filaments

Figure 10 shows the applications of 3DP in various fields according to a comprehensive industry report published by Wohlers Associates. The applications of industrial-grade 3DP are concentrated globally in five primary areas: transportation, aerospace, industrial equipment, consumer/electronic products, and medicine. In all other areas, 3DP is typically employed in the R&D stage for prototyping.

6.1 Transportation

In this field, investigations into the use of 3DP technology have been performed, for instance, to study the wear resistance of 3D-printed products [98,151]. However, the actual batch application is limited by the cost of 3DP and batch capacity. Owing to the current limitations in the types and properties of 3DP materials, plastic part production remains in the R&D stage for trial production. Metals cannot be used in large-scale batch production owing to their high cost and low production efficiency; consequently, they are limited to high-end models with improved performance. Carbon- [152]

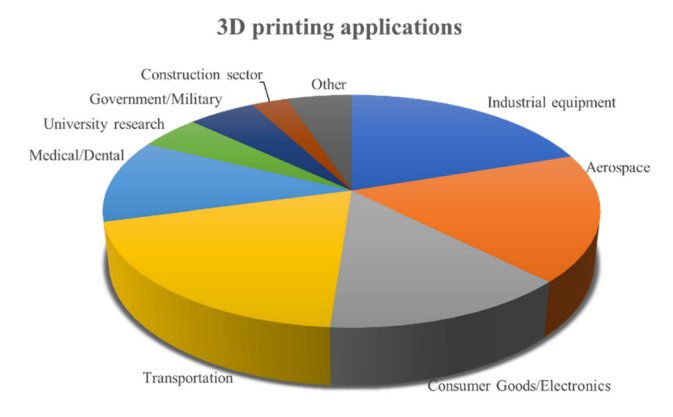


Figure 10: Applications of 3DP in various fields.

and CF-reinforced [25,33,153] PLA composites have superior tensile and bending properties compared to those of pure PLA and can also be compounded with reinforcing materials such as nanotubes and graphene [154] to improve yield strength and mechanical properties.

6.2 Aerospace applications

3DP technology can be adopted in the aerospace industry for fabricating jigs and fixtures, producing parts, and machining composite materials. The aerospace industry can develop a new fighter jet in as little as 3 years with the help of 3DP and other information technologies, which can solve design challenges and avoid expensive, time-consuming machining and production. Owing to its high flexibility, high performance, flexible manufacturing characteristics, and ability to permit free rapid prototyping of complex parts, 3DP has potential to excel in the aerospace field [98,151] and provide strong technical support for manufacturing defense equipment.

6.3 Industrial and electronic applications

The industrial sector has taken more advantage of the customization of 3DP to develop products with personalized features to appeal to different user groups. PLA can be endowed with conductive properties and improved electrical/thermal performance when combined with materials such as CNFs [115–117], conductive CB particles [105,106], and graphene [108]. In terms of electronics, 3DP can be utilized to prepare functional electromechanical components such as biosensing devices, sensors, 3D electrodes, and soft robotics components.

6.4 Medical and dental applications

Presently, the medical industry has a broad range of 3D-printed products and applications from devices and organs to surgeries. 3DP technology can be used in the medical field for surgical planning models, teaching and training, and prototyping of medical devices. Moreover, it can be used to advance the medical field by printing 3D models based on real patient imaging data to mimic various tissue properties. Additionally, it can customize medical instruments, particularly in dental/orthopedic implant fabrication and orthopedic rehabilitation [86,92,128].

3DP technology is also extensively used in fields such as consumer goods manufacturing, art, and fashion. With the continuous advances in 3DP technology – industrial or otherwise – the ensuing applications are continuing to broaden, ingraining aspects of our daily life. The future applications of 3DP technology could become an important factor in assessing the competitiveness of many industries.

7 Conclusions

FDM-based 3D-printed products have been used in various fields including packaging, transportation, and biomedical, electronic, and electrical industries. PLA, which is the most widely used raw material for 3DP, has attracted considerable research attention owing to its degradable nature. This review summarizes the literature on FDM-derived PLA materials published in the past 5 years. Pure PLA has inferior performance and cannot be readily applied in areas requiring high material performance. Consequently, it is modified to achieve superior mechanical properties and functionalities. The preparation of FDM-based 3DP PLA materials with low cost and superior overall performance using suitable modification methods must be prioritized.

Funding information: The authors are grateful for financial support from the Guangxi Natural Science Foundation [2020GXNSFAA297042], Guangxi Bossco Environmental Protection Technology (Bossco) [AA17129006], Guangxi Key Laboratory of Clean Pulp & Papermaking and Pollution Control [2021KF53], and Guangdong Basic and Applied Basic Research Foundation [2019A1515110667].

Author contributions: Yishan Li: conceptualization, Writing – review and editing, writing – original draft, project administration; Lijie Huang: investigation, funding acquisition, supervision; Xiyue Wang: methodology, formal analysis; Xuyang Lu: formal analysis, Validation; Yanan Wang: formal analysis, validation; Zhehao Wei: validation; Qi Mo: software; Yao Sheng: formal analysis; Shuya Zhang: formal analysis; Chongxing Huang: funding acquisition; Qingshan Duan: funding acquisition. All authors have accepted responsibility for the entire content of this manuscript and approved its submission.

Conflict of interest: The authors state no conflict of interest.

Data availability statement: The data that support the findings of this study are openly available in [repository name] at [URL], referencenumber [reference number].

References

- [1] Van den Eynde, M. and P. Van Puyvelde. 3D Printing of Poly(lactic acid). In: *Industrial Applications of Poly(Lactic Acid)*, M. L. DiLorenzo, Androsch, R., (Eds.), Springer international publishing AG, Germany, 2018, pp. 139–158.
- [2] Liu, Z., Y. Wang, B. Wu, C. Cui, Y. Guo, and C. Yan. A critical review of fused deposition modeling 3D printing technology in manufacturing polylactic acid parts. *The International Journal of Advanced Manufacturing Technology*, Vol. 102, No. 9–12, 2019, pp. 2877–2889.
- [3] Subramaniam, S. R., M. Samykano, S. K. Selvamani, W. K. Ngui, K. Kadirgama, K. Sudhakar, et al. 3D printing: Overview of PLA progress. AIP Conference Proceedings, Vol. 2059, No. 1, 2019, id. 020015.
- [4] Lebedev, S. M., O. S. Gefle, E. T. Amitov, D. V. Zhuravlev, D. Y. Berchuk, and E. A. Mikutskiy. Mechanical properties of PLA-based composites for fused deposition modeling technology. *The International Journal of Advanced Manufacturing Technology*, Vol. 97, No. 1–4, 2018, pp. 511–518.
- [5] Baran, E. H. and H. Y. Erbil. Surface modification of 3D printed PLA objects by fused deposition modeling: a review. *Colloids and Interfaces*, Vol. 3, No. 2, 2019, id. 43.
- [6] Yu, W., M. Li, W. Lei, Y. Pu, K. Sun, and Y. Ma. Effects of Wood Flour (WF) pretreatment and the addition of a toughening agent on the properties of FDM 3D-printed WF/Poly(lactic acid) biocomposites. *Molecules*, Vol. 27, No. 9, 2022, id. 2985.
- [7] Li, L., Y. Chen, T. Yu, N. Wang, C. Wang, and H. Wang. Preparation of polylactic acid/TEMPO-oxidized bacterial cellulose nanocomposites for 3D printing via Pickering emulsion approach. *Composites Communications*, Vol. 16, 2019, pp. 162–167.
- [8] Daver, F., K. P. M. Lee, M. Brandt, and R. Shanks. Cork-PLA composite filaments for fused deposition modelling. *Composites Science and Technology*, Vol. 168, 2018, pp. 230–237.
- [9] He, J., D. Sun, Y. Cao, and H. Lai. Blending Modification of PLA Used for Fused Deposition Modeling. *Engineering Plastics Application*, Vol. 45, No. 6, 2017, pp. 7–11.
- [10] Coppola, B., N. Cappetti, L. Di Maio, P. Scarfato, and L. Incarnato. Influence of 3D Printing Parameters on the Properties of PLA/clay Nanocomposites, 9th International Conference on times of polymers and composites: from aerospace to nanotechnology, 2018.
- [11] Coppola, B., N. Cappetti, L. Di Maio, P. Scarfato, and L. Incarnato. 3D Printing of PLA/clay nanocomposites: Influence of printing temperature on printed samples properties. *Materials*, Vol. 11, No. 10, 2018, id. 1947.
- [12] Cuiffo, M. A., J. Snyder, A. M. Elliott, N. Romero, S. Kannan, and G. P. Halada. Impact of the Fused Deposition (FDM) Printing Process on Polylactic Acid (PLA) Chemistry and Structure. *Applied Sciences-Basel*, Vol. 7, No. 6, 2017, id. 579.
- [13] Donate, R., M. Monzon, M. E. Aleman-Dominguez, and Z. Ortega. Enzymatic degradation study of PLA-based composite scaffolds. Reviews on Advanced Materials Science, Vol. 59, No. 1, 2020, pp. 170–175.
- [14] Lee, C. H., F. N. B. M. Padzil, S. H. Lee, Z.M.A.a Ainun, and L. C. Abdullah. Potential for natural fiber reinforcement in PLA Polymer Filaments for Fused Deposition Modeling (FDM) additive manufacturing: A review. *Polymers*, Vol. 13, No. 9, 2021, id. 1407.
- [15] Mazzanti, V., L. Malagutti, and F. Mollica. FDM 3D printing of polymers containing natural fillers: A review of their mechanical properties. *Polymers*, Vol. 11, No. 7, 2019, id. 1094.

- [16] Chen, L. and X. Zhang. Modification the surface quality and mechanical properties by laser polishing of Al/PLA part manufactured by fused deposition modeling. *Applied Surface Science*, Vol. 492, 2019, pp. 765–775.
- [17] Chen, L., X. Zhang, and S. Gan. Effects of laser polishing on surface quality and mechanical properties of PLA parts built by fused deposition modeling. *Journal of Applied Polymer Science*, Vol. 137, No. 3, 2020, id. 48288.
- [18] Chen, L., X. Zhang, Y. Wang, and T. A. Osswald. Laser polishing of Cu/PLA composite parts fabricated by fused deposition modeling: Analysis of surface finish and mechanical properties. *Polymer Composites*, Vol. 41, No. 4, 2020, pp. 1356–1368.
- [19] Zhang, X. and L. Chen. Effects of laser scanning speed on surface roughness and mechanical properties of aluminum/Polylactic Acid (Al/PLA) composites parts fabricated by fused deposition modeling. *Polymer Testing*, Vol. 91, 2020, id. 106785.
- [20] Yadav, D. and I. Mingareev. Utilizing ultrafast lasers for postprocessing to improve mechanical properties of 3D-printed parts. *Journal of Laser Applications*, Vol. 35, No. 1, 2023, id. 012016.
- [21] Wang, Y., Z. Liu, H. Gu, C. Cui, and J. Hao. Improved mechanical properties of 3D-printed SiC/PLA composite parts by microwave heating. *Journal of Materials Research*, Vol. 3420, 2019, pp. 3412–3419.
- [22] Rajpurohit, S. R. and H. K. Dave. Analysis of tensile strength of a fused filament fabricated PLA part using an open-source 3D printer. *The International Journal of Advanced Manufacturing Technology*, Vol. 101, No. 5–8, 2019, pp. 1525–1536.
- [23] El Magri, A., K. El Mabrouk, S. Vaudreuil, and M. E. Touhami. Mechanical properties of CF-reinforced PLA parts manufactured by fused deposition modeling. *Journal of Thermoplastic Composite Materials*, Vol. 34, No. 5, 2021, pp. 581–595.
- [24] Li, Y., Q. Dong, Q. Tai, S. Gao, H. Guan, and W. Yan. Mechanical properties of carbon fiber composite in fused deposition modeling of additive manufacturing. *Journal of Plasticity Engineering*, Vol. 24, No. 3, 2017, pp. 225–230.
- [25] Li, Y., S. Gao, R. Dong, X. Ding, and X. Duan. Additive manufacturing of PLA and CF/PLA binding layer specimens via fused deposition modeling. *Journal of Materials Engineering And Performance*, Vol. 27, No. 2, 2018, pp. 492–500.
- [26] Cui, Y., M. Jia, P. Xue, J. Jiang, and J. Cai. Research of continuous glass fiber reinforced PLA composites prepared by 3D printing technology. *China Plastics Industry*, Vol. 48, No. 1, 2020, pp. 51–5477.
- [27] Wei, Q., X. Cai, Y. Guo, G. Wang, Y. Guo, M. Lei, et al. Atomic-scale and experimental investigation on the micro-structures and mechanical properties of PLA blending with CMC for additive manufacturing. *Materials & Design*, Vol. 183, 2019, id. 108158.
- [28] Kesavarma, S., E. H. Lee, M. Samykano, K. Kadirgama, M. M. Rahman, and A. G. N. Sofiah. Flextural properties of 3D printed Copper-Filler Polylactic Acid (Cu-PLA), 5th International conference on mechanical engineering research 2019 (ICMER 2019), I.O.P. Publishing, 2020.
- [29] Selvamani, S. K., W. K. Ngui, K. Rajan, M. Samykano, R. Kumar, and A. M. Badadhe. Investigation of bending and compression properties on PLA-brass composite using FDM. *Physics and Chemistry of the Earth*, Vol. 128, 2022, id. 103251.
- [30] Zhang, X., L. Chen, T. Mulholland, and T. A. Osswald. Effects of raster angle on the mechanical properties of PLA and Al/PLA composite part produced by fused deposition modeling. *Polymers* for Advanced Technologies, Vol. 30, No. 8, 2019, pp. 2122–2135.

- [31] Gao, X., D. Zhang, S. Qi, X. Wen, and Y. Su. Mechanical properties of 3D parts fabricated by fused deposition modeling: Effect of various fillers in polylactide. *Journal of Applied Polymer Science*, Vol. 136, No. 31, 2019, id. 47824.
- [32] Cao, M., T. Cui, Y. Yue, C. Li, X. Guo, X. Jia, et al. Investigation of carbon fiber on the tensile property of FDM-produced PLA specimen. *Polymers*, Vol. 14, No. 23, 2022, id. 5230.
- [33] Heidari-Rarani, M., M. Rafiee-Afarani, and A. M. Zahedi. Mechanical characterization of FDM 3D printing of continuous carbon fiber reinforced PLA composites. *Composites Part B-Engineering*, Vol. 175, 2019, id. 107147.
- [34] Coppola, B., E. Garofalo, L. Di Maio, P. Scarfato, and L. Incarnato. Investigation on the use of PLA/hemp composites for the fused deposition modelling (FDM) 3D printing, 9th International Conference on times of polymers and composites: from aerospace to nanotechnology, 2018.
- [35] Yu, W., T. Yuan, Y. Yao, Y. Deng, and X. Wang. PLA/coffee grounds composite for 3D printing and its properties. *Forests*, Vol. 14, No. 2, 2023, id. 367.
- [36] Li, X., Z. Ni, S. Bai, and B. Lou. Preparation and mechanical properties of fiber reinforced PLA for 3D Printing Materials, 2017 International symposium on application of materials science and energy materials (SAMSE 2017), IOP, 2018.
- [37] Fekete, I., F. Ronkay, and L. Lendvai. Highly toughened blends of poly(lactic acid) (PLA) and natural rubber (NR) for FDM-based 3D printing applications: The effect of composition and infill pattern. *Polymer Testing*, Vol. 99, 2021, id. 107205.
- [38] Yang, M., N. Xiong, J. Hu, and Y. Weng. Study on Preparation and Properties of PLA/PHBV 3D-Printing Filament. *China Plastics*, Vol. 33, No. 4, 2019, pp. 6–11.
- [39] Wei, Q., D. Sun, R. Yang, Y. Wang, J. Zhang, X. Li, et al. Influence of Fused Deposition Molding Printing Process on the Toughness and Miscibility of Polylactic Acid/Polycaprolactone Blends. *Journal of Materials Engineering and Performance*, Vol. 31, No. 2, 2022, pp. 1338–1345.
- [40] Enrique Solorio-Rodriguez, L. and A. Vega-Rios. Filament Extrusion and Its 3D Printing of Poly(Lactic Acid)/Poly(Styrene-co-Methyl Methacrylate) Blends. Applied Sciences-Basel, Vol. 9, No. 23, 2019, id. 5153.
- [41] Kaygusuz, B. and S. Ozerinc. Improving the ductility of polylactic acid parts produced by fused deposition modeling through polyhydroxyalkanoate additions. *Journal of Applied Polymer Science*, Vol. 136, No. 43, 2019, id. 48154.
- [42] Han, X., L. Huang, Z. Wei, Y. Wang, H. Chen, C. Huang, et al. Technology and mechanism of enhanced compatibilization of polylactic acid-grafted glycidyl methacrylate. *Industrial Crops and Products*, Vol. 172, 2021, id. 114065.
- [43] An, Z., R. Xue, K. Ye, H. Zhao, Y. Liu, P. Li, et al. Recent advances in self-healing polyurethane based on dynamic covalent bonds combined with other self-healing methods. *Nanoscale*, Vol. 1514, 2023, pp. 6505–6520.
- [44] Li, H., J. Zhang, R. Xue, Z. An, W. Wu, Y. Liu, et al. Construction of self-healable and recyclable waterborne polyurethane-MOF membrane for adsorption of dye wastewater based on solvent etching deposition method. Separation and Purification Technology, Vol. 320, 2023, id. 124145.
- [45] Jayswal, A. and S. Adanur. Characterization of PLA/TPU composite filaments manufactured for 3D printing with FDM. *Journal of Thermoplastic Composite Materials*, Vol. 36, No. 4, 2021, pp. 1450–1471.

- [46] Li, W., X. Xia, H. Lin, Y. Yang, Q. Chen, and L. Xiao. Effect of fused deposition style on impact properties of PLA/TPU blends. *China Plastics*, Vol. 33, No. 9, 2019, pp. 21–26.
- [47] Dang, H., C. Lei, Z. Liu, and Z. Xu. Toughening modification of polylactic acid wire for 3D printing by star polyurethane. *Engineering Plastics Application*, Vol. 49, No. 1, 2021, pp. 13–19.
- [48] Ahmed, W., S. Siraj, and A. H. Al-Marzouqi. 3D printing PLA waste to produce ceramic based particulate reinforced composite using abundant silica-sand: mechanical properties characterization. *Polymers*, Vol. 12, No. 11, 2020, id. 2579.
- [49] Tao, Y., H. Wang, Z. Li, P. Li, S. Q. Shi, and W. R. Caseri. Development and application of wood flour-filled polylactic acid composite filament for 3D printing. *Materials*, Vol. 10, No. 4, 2017, id. 339.
- [50] Lei, F., Y. Zhang, X. Meng, and R. Zheng. Effect of compatibilizer POE-g-MAH on properties of PLA/wood flour composites for FDM. China Plastics Industry, Vol. 47, No. 9, 2019, pp. 38–4169.
- [51] Luo, T. and L. Sun. Effect of coupling agent on 3D printing performance of PLA/PBAT/poplar powder. *Composites, China Plastics*, Vol. 3411, 2020, pp. 66–72.
- [52] Du, J., Y. Song, Z. Zhang, Y. Fang, W. Wang, and Q. Wang. Influence of maleic anhydride/glycidyl methacrylate cografted polylactic acid on properties of wood flour/PLA composites. *Journal of Materials Engineering*, Vol. 4512, 2017, pp. 30–36.
- [53] Zhao, S., X. Gong, Z. Wang, X. Fu, X. Zhao, Z. Dai, et al. Glycidyl methacrylate grafted onto polylactic acid improving the interfacial compatibility of bamboo fiber/polylactic acid biomass composites. *Polymer Bulletin*, Vol. 11, 2018, pp. 60–67.
- [54] Rasselet, D., A.-S. Caro-Bretelle, A. Taguet, and J.-M. Lopez-Cuesta. Reactive compatibilization of PLA/PA11 blends and their application in additive manufacturing. *Materials*, Vol. 12, No. 3, 2019, id. 485
- [55] Liu, W., J. Zhou, Y. Li, J. Wang, and J. Xu. Influence of addition of ATBC on the preparation and properties of PLA/PCL filaments for FDM3D printing. *Journal of Functional Materials*, Vol. 4811, 2017, pp. 11168–11173.
- [56] Geng, Y., H. He, H. Liu, and H. Jing. Preparation of polycarbonate/ poly(lactic acid) with improved printability and processability for fused deposition modeling. *polymers for Advanced Technologies*, Vol. 3111, 2020, pp. 2848–2862.
- [57] Yang, H., C. Ye, J. Wang, G. Jia, T. Duan, S. Liu, et al. Preparation of super-toughened PLA/PCL blends via reactive compatibilization and stereocomplexation crystallization. *Engineering Plastics Application*, Vol. 5011, 2022, pp. 1–724.
- [58] Zhao, H., S. Hu, G. Li, X. Xia, Y. Zhang, and Q. Wang. Poly(adipate butylene-to-terephthalate)/Poly(lactic acid) Blend System with Aluminate Coupling Agent. *Polymer Materials Science & Engineering*, Vol. 3811, 2022, pp. 34–40.
- [59] Bustillos, J., D. Montero, P. Nautiyal, A. Loganathan, B. Boesl, and A. Agarwal. Integration of graphene in poly(lactic) acid by 3D printing to develop creep and wear-resistant hierarchical nanocomposites. *Polymer Composites*, Vol. 3911, 2018, pp. 3877–3888.
- [60] Kumar, S., R. Singh, M. Singh, T. P. Singh, and A. Batish. Multi material 3D printing of PLA-PA6/TiO(2)polymeric matrix: Flexural, wear and morphological properties. *Journal of Thermoplastic Composite Materials*, Vol. 3511, 2020, pp. 2105–2124.
- [61] Guessasma, S., S. Belhabib, and H. Nouri. Thermal cycling, microstructure and tensile performance of PLA-PHA polymer printed using fused deposition modelling technique. *Rapid Prototyping Journal*, Vol. 26, No. 1, 2020, pp. 122–133.

- [62] Cardoso, P. H. M., R. R. T. P. Coutinho, F. R. Drummond, M. D. N. da Conceicao, and R. M. D. S. M. Thire., Evaluation of Printing Parameters on Porosity and Mechanical Properties of 3D Printed PLA/PBAT Blend Parts. *Macromolecular Symposia*, Vol. 394, No. 1, 2020, id. 2000157.
- [63] Gurchetan, S., K. Ranvijay, S. Rupinder, R. Md Mustafizur, and R. Seeram. Rheological, mechanical, thermal, tribological and morphological properties of PLA-PEKK-HAp-CS composite. *Journal Of Central South University*, Vol. 28, No. 6, 2021, pp. 1615–1626.
- [64] Kumar, S., R. Singh, T. P. Singh, and A. Batish. On mechanical characterization of 3-D printed PLA-PVC-wood dust-Fe3O4 composite. *Journal Of Thermoplastic Composite Materials*, Vol. 35, No. 1, 2022, pp. 36–53.
- [65] Bakhshi, R., M. Mohammadi-Zerankeshi, M. Mehrabi-Dehdezi, R. Alizadeh, S. Labbaf, and P. Abachi. Additive manufacturing of PLA-Mg composite scaffolds for hard tissue engineering applications. *Journal Of The Mechanical Behavior Of Biomedical Materials*, Vol. 138, 2023, id. 105655.
- [66] Milenkovic, S., V. Slavkovic, C. Fragassa, N. Grujovic, N. Palic, and F. Zivic. Effect of the raster orientation on strength of the continuous fiber reinforced PVDF/PLA composites, fabricated by hand-layup and fused deposition modeling. *Composite Structures*, Vol. 270, 2021, id. 114063.
- [67] Corcione, C. E., F. Gervaso, F. Scalera, S. K. Padmanabhan, M. Madaghiele, F. Montagna, et al. Highly loaded hydroxyapatite microsphere/PLA porous scaffolds obtained by fused deposition modelling. *Ceramics International*, Vol. 45, No. 2, 2019, pp. 2803–2810.
- [68] Nevado, P., A. Lopera, V. Bezzon, M. R. Fulla, J. Palacio, M. A. Zaghete, et al. Preparation and in vitro evaluation of PLA/biphasic calcium phosphate filaments used for fused deposition modelling of scaffolds. *Materials Science & Engineering C-Materials For Biological Applications*, I.O.P. Publishing: Vol. 114, 2020, id. 111013.
- [69] Song, X., W. He, H. Qin, S. Yang, and S. Wen. Fused deposition modeling of poly (lactic acid)/macadamia composites-thermal, mechanical properties and scaffolds. *Materials*, Vol. 13, No. 2, 2020, id. 258.
- [70] Xue, Y., X. Zuo, L. Wang, Y. Zhou, Y. Pan, J. Li, et al. Enhanced flame retardancy of poly(lactic acid) with ultra-low loading of ammonium polyphosphate. *Composites Part B-Engineering*, Vol. 196, 2020, id. 108124.
- [71] Zerankeshi, M. M., S. S. Sayedain, M. Tavangarifard, and R. Alizadeh. Developing a novel technique for the fabrication of PLA-graphite composite filaments using FDM 3D printing process. Ceramics International, Vol. 4821, 2022, pp. 31850–31858.
- [72] Vardhan, H., R. Kumar, and J. S. Chohan. Investigation of tensile properties of sprayed aluminium based PLA composites fabricated by FDM technology. *Materials Today-Proceedings*, Vol. 33, 2020, pp. 1599–1604.
- [73] Tumer, E. H. and H. Y. Erbil. Extrusion-based 3D printing applications of PLA composites: A review. *Coatings*, Vol. 11, No. 4, 2021, id. 390.
- [74] Liu, W., N. Wu, and K. Pochiraju. Shape recovery characteristics of SiC/C/PLA composite filaments and 3D printed parts. *Composites Part A-Applied Science And Manufacturing*, Vol. 108, 2018, pp. 1–11.
- 75] Wang, Y., Y. Wang, Q. Wei, J. Zhang, M. Lei, M. Li, et al. Effects of the composition ratio on the properties of PCL/PLA blends: a kind of thermo-sensitive shape memory polymer composites. *Journal Of Polymer Research*, Vol. 28, No. 12, 2021, No. 12, id. 451.

- [76] Hua, D., X. Zhang, Z. Ji, C. Yan, B. Yu, Y. Li, et al. 3D printing of shape changing composites for constructing flexible paper-based photothermal bilayer actuators. Journal Of Materials Chemistry C, Vol. 6, No. 8, 2018, pp. 2123-2131.
- [77] Lin, C., L. Liu, Y. Liu, and J. Leng. 4D printing of shape memory polybutylene succinate/polylactic acid (PBS/PLA) and its potential applications. Composite Structures, Vol. 279, 2022, id. 114729.
- Dezaki, M. L. and M. Bodaghi. Sustainable 4D printing of magneto-electroactive shape memory polymer composites. International Journal Of Advanced Manufacturing Technology, Vol. 126, 2023, pp. 35-48.
- Chen, X., G. Chen, G. Wang, P. Zhu, and C. Gao. Recent progress on 3D-printed polylactic acid and its applications in bone repair. Advanced Engineering Materials, Vol. 22, No. 4, 2020, id. 1901065.
- Guerra, A. J., P. Cano, M. Rabionet, T. Puig, and J. Ciurana. 3D-Printed PCL/PLA composite stents: towards a new solution to cardiovascular problems. *Materials*, Vol. 11, No. 6, 2018, id. 1679.
- [81] Mystiridou, E., A. C. Patsidis, and N. Bouropoulos. Development and characterization of 3D printed multifunctional bioscaffolds Based on PLA/PCL/HAp/BaTiO3 composites. Applied Sciences-Basel, Vol. 11, No. 9, 2021, id. 4253.
- Najera, S. E., M. Michel, and N.-S. Kim. 3D Printed PLA/PCL/TiO2 [82] composite for bone replacement and grafting. MRS Advances, Vol. 340, 2018, pp. 2373-2378.
- [83] Olam, M. and N. Tosun. 3D-printed polylactide/hydroxyapatite/ titania composite filaments. Materials Chemistry And Physics, Vol. 276, 2022, id. 125267.
- Olam, M. and N. Tosun. Assessment of 3D printings produced in [84] fused deposition modeling printer using polylactic Acid/TiO2/ hydroxyapatite composite filaments. Journal of Materials Engineering And Performance, Vol. 31, No. 6, 2022, pp. 4554-4565.
- Fan, Z.-w, X.-y Zhao, S. Qiu, Y. Wang, J. Guo, H.-x Quan, et al. 3D printing of polylactic acid/poly ethylene glycol/hydroxyapatite porous bone scaffolds and their biocompatibility. Cailiao Gongcheng-Journal of Materials Engineering, Vol. 49, No. 4, 2021,
- Wang, W., B. Zhang, M. Li, J. Li, C. Zhang, Y. Han, et al. 3D printing of PLA/n-HA composite scaffolds with customized mechanical properties and biological functions for bone tissue engineering. Composites Part B-Engineering, Vol. 224, 2021, id. 109192.
- Wang, W., B. Zhang, L. Zhao, M. Li, Y. Han, L. Wang, et al. [87] Fabrication and properties of PLA/nano-HA composite scaffolds with balanced mechanical properties and biological functions for bone tissue engineering application. Nanotechnology Reviews, Vol. 10, No. 1, 2021, pp. 1359-1373.
- Salamanca, E., T.-C. Tsao, H.-W. Hseuh, Y.-F. Wu, C.-S. Choy, C.-K. Lin, et al. Fabrication of polylactic acid/beta-tricalcium phosphate FDM 3D printing fiber to enhance osteoblastic-like cell performance. Frontiers In Materials, Vol. 8, 2021, id. 683706.
- [89] Jiang, G., T. Yang, J. Xu, D. Tao, C. Luo, C. Wang, et al. Investigation into hydroxypropyl-methylcellulose-reinforced polylactide composites for fused deposition modelling. Industrial Crops And Products, Vol. 146, 2020, id. 112174.
- Kohan, M., S. Lancos, M. Schnitzer, J. Zivcak, and R. Hudak. [90] Analysis of PLA/PHB biopolymer material with admixture of hydroxyapatite and tricalcium phosphate for clinical use. Polymers, Vol. 14, No. 24, 2022, id. 5357.
- Yang, F., X. Ye, J. Zhong, Z. Lin, S. Wu, Y. Hu, et al. Recycling of waste crab shells into reinforced poly (lactic acid) biocomposites

- for 3D printing. International Journal of Biological Macromolecules, Vol. 234, 2023, pp. 122974-122974.
- [92] Manjunath, K. S., K. Sridhar, V. Gopinath, K. Sankar, A. Sundaram, N. Gupta, et al. Facile manufacturing of fused deposition modelled composite scaffold for tissue engineering - An embedment model with plasticity for incorporation of additives. Biomedical materials (Bristol, England), Vol. 16, 2020, id. 015028.
- [93] Lett, I. A., S. Sagadevan, S. Paiman, F. Mohammad, R. Schirhagl, E. Leonard, et al. Exploring the thumbprints of Ag-hydroxyapatite composite as a surface coating bone material for the implants. Journal of Materials Research and Technology-Jmr&T, Vol. 9, No. 6, 2020, pp. 12824-12833.
- Reina, S. A., B. J. E. Tito, M. H. Malini, F. G. Igrimatien, and E. Sa'divah, Aminatun, Porosity and compressive strength of PLAbased scaffold coated with hydroxyapatite-gelatin to reconstruct mandibula: a literature review. Journal of Physics: Conference Series, Vol. 1816, 2021, id. 012085.
- [95] Zhang, C., M. Wang, J. Zhang, B. Zou, and Y. Wang. Self-template synthesis of mesoporous and biodegradable Fe3O4 nanospheres as multifunctional nanoplatform for cancer therapy. Colloids and surfaces B, Biointerfaces, Vol. 229, 2023, pp. 113467-113467.
- [96] Yao, R., H. Wang, R. Shan, L. Liu, Y. Zhao, Y. Sun, et al. Biodegradable porous Zn-1Mg-3 beta TCP scaffold for bone defect repair: In vitro and in vivo evaluation. Journal of Materials Science & Technology, Vol. 162, 2023, pp. 189-202.
- [97] Scaffaro, R., A. Maio, E. F. Gulino, G. Alaimo, and M. Morreale. Green composites based on PLA and agricultural or marine waste prepared by FDM. Polymers, Vol. 13, No. 9, 2021, id. 1361.
- **[98]** Ertane, E. G., A. Dorner-Reisel, O. Baran, T. Welzel, V. Matner, and S. Svoboda. Processing and wear behaviour of 3D printed PLA reinforced with biogenic carbon. Advances in Tribology, Vol. 2018, 2018, id. 1763182.
- [99] Hanumantharaju, H. G., K. P. Prashanth, B. Ramu, N. Venkatesh, and G. R. Chethan. 3D printing of biopolymer composites investigation on effect of egg shell particles on polylactic acid matrix. Biointerface Research In Applied Chemistry, Vol. 13, 2023, No. 9,
- [100] Salehi, S., H. Ghomi, S. A. Hassanzadeh-Tabrizi, N. Koupaei, and M. Khodaei. The effect of polyethylene glycol on printability, physical and mechanical properties and osteogenic potential of 3D-printed poly (L-lactic acid)/polyethylene glycol scaffold for bone tissue engineering. International Journal of Biological Macromolecules, Vol. 221, 2022, pp. 1325-1334.
- Quader, R., E. Dramko, D. Grewell, J. Randall, and L. K. Narayanan. Characterizing the Effect of Filament Moisture on Tensile Properties and Morphology of Fused Deposition Modeled Polylactic Acid/Polybutylene Succinate Parts. 3d Printing And Additive Manufacturing, 2023.
- [102] Kariz, M., M. Sernek, and M. K. Kuzman. Effect of humidity on 3D-Printed Specimens From Wood-PLA FILAMENTS. Wood Research, Vol. 63, No. 5, 2018, pp. 917-922.
- [103] Tomec, D. K., A. Straze, A. Haider, and M. Kariz. Hygromorphic response dynamics of 3D-printed wood-PLA composite bilayer actuators. Polymers, Vol. 13, No. 19, 2021, id. 3209.
- [104] Zheng, Y., L. Xiao, X. Xia, C. Cao, X. Liu, Q. Qian, et al. The study of the preparation and adsorption application of PLA/PBS/camellia seed powder composites based on 3D printing. China Plastics Industry, Vol. 49, No. 6, 2021, pp. 153-158.

- [105] Sathies, T., P. Senthil, and C. Prakash. Application of 3D printed PLA-carbon black conductive polymer composite in solvent sensing. *Materials Research Express*, Vol. 6, No. 11, 2019, id. 115349.
- [106] Tirado-Garcia, I., D. Garcia-Gonzalez, S. Garzon-Hernandez, A. Rusinek, G. Robles, J. M. Martinez-Tarifa, et al. Conductive 3D printed PLA composites: On the interplay of mechanical, electrical and thermal behaviours. *Composite Structures*, Vol. 265, 2021, id. 113744.
- [107] Stefano, J. S., L. R. Guterres, E. Silva, and B. C. Janegitz. New carbon black-based conductive filaments for the additive manufacture of improved electrochemical sensors by fused deposition modeling. *Microchimica Acta*, Vol. 189, No. 11, 2022, id. 414.
- [108] Daniel, F., N. H. Patoary, A. L. Moore, L. Weiss, and A. D. Radadia. Temperature-dependent electrical resistance of conductive polylactic acid filament for fused deposition modeling. *International Journal Of Advanced Manufacturing Technology*, Vol. 99, No. 5–8, 2018, pp. 1215–1224.
- [109] Tan, D. K., A. Nokhodchi, and N. Munzenrieder. Fabrication of flexible and transferable RTDs via fused deposition modelling 3D printing. *IEEE International Conference on Flexible and Printable* Sensors and Systems (FLEPS), Vol. 2021, 2021, pp. 4.
- [110] Kim, H. and S. Lee. Characterization of electrical heating performance of CFDM 3D-Printed Graphene/Polylactic Acid (PLA) horseshoe pattern with different 3d printing directions. *Polymers*, Vol. 12, No. 12, 2020, id. 2955.
- [111] Kim, H. and S. Lee. Electrical heating performance of graphene/ PLA-based various types of auxetic patterns and its composite cotton fabric manufactured by CFDM 3D printer. *Polymers*, Vol. 13, No. 12, 2021, id. 2010.
- [112] Ivanov, E., R. Kotsilkova, H. Xia, Y. Chen, R. K. Donato, K. Donato, et al. PLA/Graphene/MWCNT Composites with Improved Electrical and thermal properties suitable for FDM 3D printing applications. *Applied Sciences-Basel*, Vol. 9, No. 6, 2019, id. 1209.
- [113] Lamberti, P., G. Spinelli, P. P. Kuzhir, L. Guadagno, C. Naddeo, V. Romano, et al. Evaluation of Thermal and Electrical Conductivity of Carbon-based PLA Nanocomposites for 3D Printing, Vol. 1981, 2018.
- [114] Luo, J., H. Wang, D. Zuo, A. Ji, and Y. Liu. Research on the application of MWCNTs/PLA composite material in the manufacturing of conductive composite products in 3D printing. *Micromachines*, Vol. 9, No. 12, 2018, id. 635.
- [115] Hernandez, J. A., C. Maynard, D. Gonzalez, M. Viz, C. Brien, J. Garcia, et al. The development and characterization of carbon nanofiber/polylactic acid filament for additively manufactured piezoresistive sensors. *Additive Manufacturing*, Vol. 58, 2022, id. 102948.
- [116] Hernandez, J. A., C. M. Maynard, D. Gonzalez, M. Viz, J. Garcia, B. Newell, et al. On the performance of additively manufactured CNF/PLA piezoresistive strain sensors, Vol. 11591, 2021.
- [117] Maynard, C. M., J. A. Hernandez, D. Gonzalez, T. N. Tallman, J. Garcia, and B. Newell. The Effect of Extrusion Temperature and Cycles on Electrical Resistivity in Carbon Nanofiber-Modified PLA Filament for Multi-Functional Additive Manufacturing, Vol. 11379, 2020.
- [118] Ye, X., C. Yang, P. Yang, Q. Gao, D. Ding, E. He, et al. Study on electromagnetic wave absorption properties of graphene/FeSiAl/ polylactic acid composites prepared by fused deposition modeling. *Journal of Materials Research*, Vol. 38, No. 6, 2023, pp. 1620–1633.
- [119] Amirov, A., A. Omelyanchik, D. Murzin, V. Kolesnikova, S. Vorontsov, I. Musov, et al. 3D printing of PLA/magnetic ferrite

- composites: effect of filler particles on magnetic properties of filament. *Processes*, Vol. 10, No. 11, 2022, id. 2412.
- [120] Ye, X., C. Yang, E. He, P. Yang, Q. Gao, T. Yan, et al.
 Electromagnetic wave absorption properties of the FeSiAl/PLA
 and FeSiAl-MoS2-Graphene/PLA double-layer absorber formed by
 fused deposition modeling. *Journal of Magnetism and Magnetic Materials*, Vol. 565, 2023, id. 170280.
- [121] Ye, X., Q. Gao, E. He, C. Yang, P. Yang, T. Yan, et al. Graphene/carbonyl iron powder composite microspheres enhance electromagnetic absorption of 3D printing composites. *Journal of Alloys and Compounds*, Vol. 937, 2023, id. 168443.
- [122] Yang, L., X. Liu, Y. Xiao, B. Liu, Z. Xue, and Y. Wang. Additive manufacturing of carbon nanotube/polylactic acid films with efficient electromagnetic interference shielding and electrical heating performance via fused deposition modeling. *Synthetic Metals*, Vol. 293, 2023, id. 117258.
- [123] Wang, Y., Z.-W. Fan, H. Zhang, J. Guo, D.-X. Yan, S. Wang, et al. 3D-printing of segregated carbon nanotube/polylactic acid composite with enhanced electromagnetic interference shielding and mechanical performance. *Materials & Design*, Vol. 197, 2021, id. 109222.
- [124] Beniak, J., L. Soos, P. Krizan, M. Matus, and V. Ruprich. Resistance and strength of conductive PLA processed by FDM additive manufacturing. *Polymers*, Vol. 14, No. 4, 2022, id. 678.
- [125] Egiziano, L., P. Lamberti, G. Spinelli, V. Tucci, R. Kotsilkova, S. Tabakova, et al. Morphological, rheological and electrical study of PLA reinforced with carbon-based fillers for 3D Printing Applications, 9th International Conference on times of polymers and composites: from aerospace to nanotechnology, 2018.
- [126] Zhao, G., H.-Y. Liu, X. Cui, X. Du, H. Zhou, Y.-W. Mai, et al. Tensile properties of 3D-printed CNT-SGF reinforced PLA composites. Composites Science And Technology, Vol. 230, 2022, id. 109333.
- [127] Yang, L., S. Li, X. Zhou, J. Liu, Y. Li, M. Yang, et al. Effects of carbon nanotube on the thermal, mechanical, and electrical properties of PLA/CNT printed parts in the FDM process. *Synthetic Metals*, Vol. 253, 2019, pp. 122–130.
- [128] Rebaioli, L., C. Pagano, and I. Fassi. Fabrication of Pla/Cnt Composite Scaffolds by Fused Deposition Modeling. Proceedings of the ASME International design engineering technical conferences and computers and information in engineering conference, 2018.
- [129] Mohapatra, A., N. Divakaran, Y. Alex, P. V. A. Kumar, and S. Mohanty. The significant role of CNT-ZnO core-shell nanostructures in the development of FDM-based 3D-printed triboelectric nanogenerators. *Materials Today Nano*, Vol. 22, 2023, id. 100313.
- [130] Mauricio Cobos, C., L. Garzon, J. Lopez-Martinez, O. Fenollar, and S. Ferrandiz. Study of thermal and rheological properties of PLA loaded with carbon and halloysite nanotubes for additive manufacturing. *Rapid Prototyping Journal*, Vol. 25, No. 4, 2019, pp. 738–743.
- [131] Cobos, C. M., O. Fenollar, J. Lopez Martinez, S. Ferrandiz, and L. Garzon. Effect of Maleinized Linseed Oil (MLO) on thermal and rheolological properties of PLA/MWCNT and PLA/HNT nanocomposites for additive manufacturing. *Rapid Prototyping Journal*, Vol. 26, No. 6, 2020, pp. 1027–1033.
- [132] Lage-Rivera, S., A. Ares-Pernas, J. C. Becerra Permuy, A. Gosset, and M.-J. Abad. Enhancement of 3D printability by FDM and electrical conductivity of PLA/MWCNT filaments using lignin as bio-dispersant. *Polymers*, Vol. 15, No. 4, 2023, id. 999.
- [133] Guo, R., Z. Ren, H. Bi, M. Xu, and L. Cai. Electrical and thermal conductivity of Polylactic Acid (PLA)-based biocomposites by

- incorporation of nano-graphite fabricated with fused deposition modeling. *Polymers*, Vol. 11, No. 3, 2019, id. 549.
- [134] Kim, M., J. H. Jeong, J.-Y. Lee, A. Capasso, F. Bonaccorso, S.-H. Kang, et al. Electrically Conducting and Mechanically Strong Graphene-Polylactic Acid Composites for 3D Printing. ACS applied materials & interfaces, Vol. 11, No. 12, 2019, pp. 11841–11848.
- [135] Vidakis, N., M. Petousis, K. Savvakis, A. Maniadi, and E. Koudoumas. A comprehensive investigation of the mechanical behavior and the dielectrics of pure polylactic acid (PLA) and PLA with graphene (GnP) in fused deposition modeling (FDM). International Journal of Plastics Technology, Vol. 23, No. 2, 2019, pp. 195–206.
- [136] Wang, Y., M. Lei, Q. Wei, Y. Wang, J. Zhang, Y. Guo, et al. 3D printing biocompatible I-Arg/GNPs/PLA nanocomposites with enhanced mechanical property and thermal stability. *Journal Of Materials Science*, Vol. 55, No. 12, 2020, pp. 5064–5078.
- [137] Kumar, S. D., K. Venkadeshwaran, and M. K. Aravindan. Fused deposition modelling of PLA reinforced with cellulose nanocrystals. *Materials Today-Proceedings*, Vol. 33, 2020, pp. 868–875.
- [138] Zhang, Q., L. Ma, X. Zhang, L. Zhang, and Z. Wang. Lignocellulose nanofiber/polylactic acid (LCNF/PLA) composite with internal lignin for enhanced performance as 3D printable filament. *Industrial Crops and Products*, Vol. 178, 2022, id. 114590.
- [139] Lu, Y., J. Xu, Y. Chen, Z. Wang, and J. Ma. Effect of KH550 on properties of PLA based 3D printing wire with high MNC content. *Transaction of China Pulp and Paper*, Vol. 34, No. 2, 2019, pp. 14–19.
- [140] Wang, Z., J. Xu, Y. Lu, L. Hu, Y. Fan, J. Ma, and et al. Preparation of 3D printable micro/nanocellulose-polylactic acid (MNC/PLA) composite wire rods with high MNC constitution. *Industrial Crops And Products*, Vol. 109, 2017, pp. 889–896.
- [141] Maroti, P., B. Kocsis, A. Ferencz, M. Nyitrai, and D. Lorinczy. Differential thermal analysis of the antibacterial effect of PLA-based materials planned for 3D printing. *Journal Of Thermal Analysis And Calorimetry*, Vol. 139, No. 1, 2020, pp. 367–374.
- [142] Bayraktar, I., D. Doganay, S. Coskun, C. Kaynak, G. Akca, and H. E. Unalan. 3D printed antibacterial silver nanowire/polylactide nanocomposites. *Composites Part B*, Vol. 172, 2019, pp. 671–678.
- [143] Tzounis, L., P. I. Bangeas, A. Exadaktylos, M. Petousis, and N. Vidakis. Three-Dimensional printed Polylactic Acid (PLA) surgical retractors with sonochemically immobilized silver nanoparticles: The next generation of low-cost antimicrobial surgery equipment. *Nanomaterials*, Vol. 10, No. 5, 2020, id. 985.

- [144] Ekonomou, S. I., S. Soe, and A. C. Stratakos. An explorative study on the antimicrobial effects and mechanical properties of 3D printed PLA and TPU surfaces loaded with Ag and Cu against nosocomial and foodborne pathogens. *Journal of the Mechanical Behavior of Biomedical Materials*, Vol. 137, 2023, id. 105536.
- [145] Balamurugan, K., M. V. Pavan, S. K. A. Ali, and G. Kalusuraman. Compression and flexural study on PLA-Cu composite filament using FDM. *Materials Today-Proceedings*, Vol. 44, 2021, pp. 1687–1691.
- [146] Coppola, B., N. Cappetti, L. Di Maio, P. Scarfato, and L. Incarnato. Layered silicate reinforced polylactic acid filaments for 3D printing of polymer nanocomposites. 2017 IEEE 3RD International Forum On Research And Technologies For Society And Industry (RTSI), IEEE: 2017, pp. 277–280.
- [147] Zhang, B., L. Wang, P. Song, X. Pei, H. Sun, L. Wu, et al. 3D printed bone tissue regenerative PLA/HA scaffolds with comprehensive performance optimizations. *Materials & Design*, Vol. 201, 2021, id. 109490.
- [148] Seng, C. T., S. Y. A. L. E. Noum, S. K. A. L. Sivanesan, and L.-J. Yu. Reduction of Hygroscopicity of PLA Filament for 3D Printing by Introducing Nano Silica as Filler, 13th International engineering research conference (13th Eureca 2019), 2020.
- [149] Ramachandran, M. G. and N. Rajeswari. Influence of nano silica on mechanical and tribological properties of additive manufactured PLA bio nanocomposite. *Silicon*, Vol. 14, No. 2, 2022, pp. 703–709.
- [150] Lee, K.-M., H. Park, J. Kim, and D.-M. Chun. Fabrication of a superhydrophobic surface using a fused deposition modeling (FDM) 3D printer with poly lactic acid (PLA) filament and dip coating with silica nanoparticles. *Applied Surface Science*, Vol. 467, 2019, pp. 979–991.
- [151] Muntean, R., S. Ambrus, N. A. Sirbu, and I.-D. Utu. Tribological Properties of Different 3D printed PLA filaments. *Nano Hybrids and Composites*, Vol. 36, 2022, pp. 103–111.
- [152] Guduru, K. K. and G. Srinivasu. Effect of post treatment on tensile properties of carbon reinforced PLA composite by 3D printing. *Materials Today-Proceedings*, Vol. 33, 2020, pp. 5403–5407.
- [153] Kumar, M. A., M. S. Khan, and S. B. Mishra. Effect of fused deposition machine parameters on tensile strength of printed carbon fiber reinforced PLA thermoplastics. *Materials Today-Proceedings*, Vol. 27, 2020, pp. 1505–1510.
- [154] Mei, H., X. Yin, J. Zhang, and W. Zhao. Compressive properties of 3D printed polylactic acid matrix composites reinforced by short fibers and SiC nanowires. Advanced Engineering Materials, Vol. 21, No. 5, 2019, id. 1800539.